SUBMILLIMETER ARRAY TECHNICAL MEMORANDUM

NUMBER : 51
SUBJECT : Analysis of the reflector back-up structure
DATE : September 30, 1991
FROM : Philippe Raffin

This report describes the reflector back-up structure for the SMA 6-meter antennas and gives its performances under mechanical and thermal loads. They are summarized in appendix 18.

1. Description of the Reflector

1.1. The primary mirror (M1) panels.

The BUS (back-up structure) allows the use of 2 types of panels, aluminum or CFRP (Carbon Fiber Reinforced Plastics) although this report shows only the influence of aluminum panels. Choosing CFRP panels would require smaller cross sections for the BUS struts, due to their smaller deadweight (8kg/m^2 for CFRP panels, based on IRAM 15m.antennas versus 30kg/m^2 for Al panels, based on the BIMA antennas).
For the aluminum panel case, there are 4 rings of panels, 12 panels for the 2 innermost rings, 24 for the 2 outermost. If CFRP is to be chosen for the panels, the BUS can accommodate 2 rings of panels, with 12 panels for the inner one and 24 for the outer one. The BUS could then provide 6 support points per panel as for the SMT.
The panels are not part of the structural model. They are supposed to be supported at their 4 corners and to introduce in the BUS only forces due to their deadweight and wind.

1.2. The secondary mirror (M2) support.

M2 is also not modeled. It is supposed to be supported in its center (Fig.1) by a rod joining the upper and lower parts of the support. The weight of M2 including the wobbling system is 50 kg and is distributed on the 2 nodes of this rod. The quadrupod supports M2 and its feet are attached to the 3rd ring of the BUS at ±45° according to the elevation axis, at the nodes C_{45}, C_{135}, C_{225} and C_{315} (Fig.2). This configuration leads to a power loss of 7.7% considering that the spar cross section is 50 mm wide by 220 mm long. The spars and the rods constituting M2-support are made out of high tensile CFRP. The spars are modeled as 3D-beam elements.

Quadrupod legs :

length	3500 mm
cross section, rectangular tube	1972 mm^2
width	50 mm
height	220 mm
thickness	4 mm
inner corner radius	16 mm

1.3. The back-up structure (BUS).

The layout is a framework made of CFRP struts with steel end-fittings connected by the way of steel ball-joints. The struts connecting the 2 layers of radial and circumferential struts, so-called pyramids, go throughout the dish, and are connected at their center to a steel hub. (Fig.3). A steel circular element connects the upper (when the dish looks at zenith) layer of struts together. Steel is essential here to maintain a good thermal behavior in the dish. (See &3.4)
The lower part of the BUS is a steel hub which is a welded box-type structure.
The CFRP struts connecting the 2 steel pieces (struts AU, UK and KV) have relatively large cross sections and therefore could be replaced by composite honeycomb sandwich plates providing an equivalent stiffness to the structure and a similar thermal behavior. The cross sections of the struts are given in Table1. These values can be further optimized in order to have fewer different tubes according to the manufacturing technique.

STRUT	CR REF	CROSS SECTION (mm2)	ROD LENGTH (mm)	number of rods	CTE_{equi} x 10^{-6} m/m/°C
AB-00	1	1200	750.5	24	2.64
AB-45	28	1200			
BC-00	2	900	748.6	24	2.64
BC-45	29	900			
CD-00	3	450	746.5	24	2.65
CD-45	30	400			
DE-00	35	200	744.2	24	2.66
DE-45	40	200			
WX-00	16	600	1068.8	24	1.94
WX-45	31	730			
XY-00	14	380	798.8	24	2.50
XY-45	32	380			
YZ-00	15	200	757.9	24	2.62
YZ-45	33	200			
BB	5	270	261.7	24	7.01
CC	4	460	450.7	24	4.19
DD	6	200	631.6	24	3.08
EE	41	200	803.2	24	2.49
XX	23	230	450.7	24	4.19
YY	7	200	631.6	24	3.08
ZZ	13	200	803.2	24	2.49
AU	18	900	570.9	24	3.37
UK	17	1300	680.5	24	2.88
KV	9	1800	622.8	24	3.12
VB	36	150	697.8	48	2.82
BX	8	150	873.5	48	2.31
XC	37	150	686.2	48	2.86

CY	10	150	784.1	48	2.54
YD	38	150	615.8	48	3.15
DZ	12	150	762.9	48	2.60
ZE-00	39	100	641.8	48	3.03
ZE-45	34	100			

Table 1.

The total length of rods (between nodes center) is 519.5 m for 744 struts including the steel end fittings and the diameter of the ball joints.
The total length of CFRP will then be about 519.5 - 744 * 0.150 = 408.m

13 different cross sections are used in this design :

area (mm^2)	total length (m)
100	30.8
150	212.2
200	104.9
230	10.8
270	6.3
380	19.2
450	17.9
460	10.8
600	25.7
900	31.7
1200	18.0
1300	16.3
1800	14.9

The material properties used for the elements are

	CFRP	STEEL
Young's modulus (GPa)	130.	207.
density (kg/m^3)	1550.	7820.

1.4. The Ring

The ring is also a welded steel box-type structure and supports the BUS. It is an interface between the mount and the reflector. It is connected to the 2 elevation bearings and to the elevation drive (Figures 4 and 5)
It is composed of 2 circular platforms connected by an inner and an outer cylinder and stiffened by bulkheads. There are local reinforcements located around the 4 areas where the connections to the hub are located, as well as in the area of the connections with the elevation drive and bearings.
This structure can be further optimized in order to reduce its weight without reducing its stiffness for instance by increasing the diameter of the inner cylinder, reducing then the 2 circular platforms.

1.5. Interface BUS/ring

In order not to destroy the homological behavior of the reflector, a special connection has to be provided between the reflector and the ring. At ±45° according to the elevation axis, 4 elements allowing only radial deformations of the hub are installed, for both mechanical and thermal loads.

1.6. Interface ring/mount, boundary conditions.

Where the ring is connected onto the elevation bearings all translations are fixed and all rotations are free. The elevation drive is modeled as a stiff rod whose position varies according to the elevation angle. Then, 5 different FEM models are used in order to represent the 5 configurations computed (0, 30, 50, 70 and 90°). The lower end of the drive is fixed for translations and free for rotations. The connections from the elevation axis to the ring, and from the ring to the drive are modeled as stiff beams.

2. Design major critical points

The major critical points of the design of the SMA 6m antennas are the following :

2.1 surface accuracy

The high surface accuracy of the reflector requires an investigation of all mechanical (gravity and wind) as well as thermal induced deformations.

2.2 pointing accuracy

The high specification of the pointing accuracy requires a careful design of the secondary support, especially for wind loads.

2.3 path length stability

The antennas are part of an array and each element of the array may not withstand the same loads at the same time, their deformation will then be different which means a difference in the path length.

3. Analysis

3.1 Programs used

I-Deas the finite element package from SDRC is used for modeling, solving and post-processing. I-Deas FEM module allows interfaces to some external solvers such as MCS/Nastran, Cosmic/Nastran, Ansys and Abaqus.

For the BFP (best fit paraboloid) calculations, a program written at IRAM for the design of the 15m. antennas of the Plateau de Bure interferometer, France and SEST, Chile is used. [1]
∂, The measured error between the deformed paraboloid and the BFP, is taken as half the phase path error between actual and expected path.

3.2 Reference system

Fig.1 shows the coordinate system used for the structural analysis of the reflector related to the nodal displacements. This coordinate system is linked to the reflector and turns in elevation with it. The origin of the system is the vertex of the paraboloid.

z-axis = outward along the boresight axis,
y-axis = perpendicular to the elevation axis so that the gravity vector is along +y when the dish points towards horizon
x-axis = so that (x,y,z) is right.

The coordinate system used for the parameters of the BFP is rotated by 180° about the boresight axis. The tables summarizing the BFP results for each mechanical or thermal loadcase refer to the latter.

3.3 Static analysis
3.3.1 Gravity

The total mass applied to the structure is about 4300 kg. at -345 mm from the vertex and is distributed as follow :

	mass(kg)	c.g. dist. from vertex (mm)
M1	880.	264.
cladding	140.	-400.
M2+wobb	50.	2639.
quad legs	43.	1717.
front struts	97.	121.
rear struts	57.	-419.
pyramids	54.	-12.
ball joints	1320.	-150.
hub cfrp	94.	-427.
hub steel	775.	-701.
ring	817.	-1310.

In this table, the weight of the steel end-fittings is not part of the CFRP struts, but is part of the ball joints. Each node has then its own deadweight, as the end-fitting is designed for each type of strut. The following table shows the values used for the calculations. They are based on IRAM 15m. steel ball joints.

	FRONT				REAR		
node	B	C	D	E	X	Y	Z
mass (kg)	10	9	8	7	8	7	6

2 gravity cases are computed : the reflector looking at zenith and at horizon. Appendixes 1 and 2 show the deformed structures with magnified deformations, appendix 3 show the residual deviations from BFP and appendix 4 show the characteristics of the BFP.

When aligning the primary mirror at an intermediate elevation and considering the range (20, 90°) of elevation , one finds [2]:

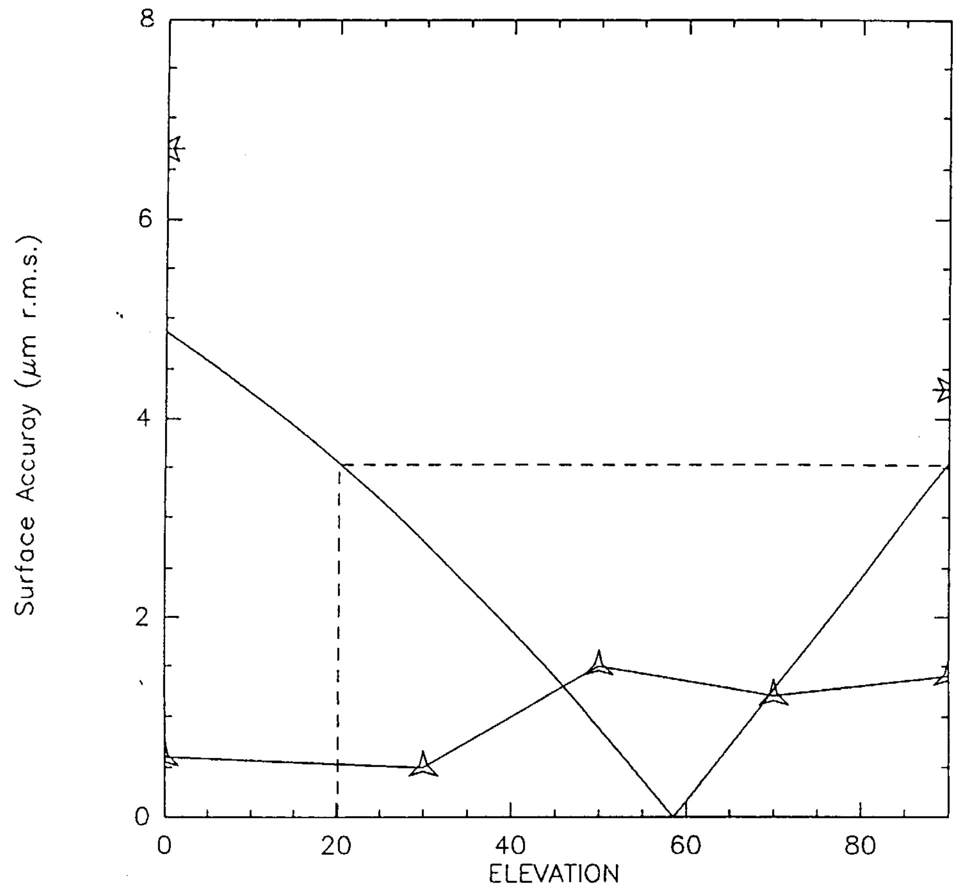

$$H(El) = \sqrt{H_{90}^2 (\sin El - \sin El_0)^2 + H_o^2 (\cos El - \cos El_0)^2}$$

H_0 = 6.7 µm r.m.s.
H_{90} = 4.3 µm r.m.s.
El_0 = 58°

El_0 is determined so that for the 2 extreme elevations (here 20 and 90°) the surface accuracy is the same, but can very well be chosen differently. The above graph rms=f(El) would simply be shifted to one side or another, favoring either the higher or lower elevations.

3.3.2. Wind

Specifications :
-altitude at Mauna Kea = 4200m, p/p_0 = 0.65478
-nominal wind speed, v = 14m/s
-dynamic pressure of wind, $q = 1/2 \cdot p \cdot v^2$ = 78.6 N/m²

5 wind loadcases are computed. We consider a front wind at 5 different elevations : 0, 30, 50, 70 and 90°. Wind forces are distributed on the primary mirror panels and the rear cladding of the reflector at the structural nodes.
Pressure distributions from wind tunnel tests used for the IRAM 30mRT of Pico Veleta, Spain (f/d=0.35) are scaled down and used.

Forces are also distributed on the quadrupod spars according to their angle to the wind direction.
A load constant with elevation is applied to the secondary mirror support. After completion of the design of this support, more detailed analysis of the wind loads on M2-support can be done and design parameters adjusted so as to maintain or improve the pointing performance of the reflector under wind loads.

Appendixes 5 to 9 show the magnified deformed structure for the 5 loadcases, appendix 10 show the corresponding residual deviations from BFPs and app.11 show their characteristics. The following table summarizes the results as far as surface accuracy, pointing and path length error are concerned.

elevation angle	Surface accuracy (µm rms)	pointing error (arc sec.)	Focus error (µm)	Path length error (µm)	loadcase Nr.
00	0.6	-0.5	66	10	3
30	0.5	-1.9	57	8	4
50	1.5	-1.7	53	7	5
70	1.2	-0.2	24	4	6
90	1.4	-1.0	16	3	7

3.4 Thermal analysis

The coefficient of thermal expansion (CTE) is 12 x10^{-6} /°C for steel, and is proportional to the length of the CFRP struts, as we consider that all the CFRP rods have end-fittings of the same length (150mm).

$$CTE_{equi} = CTE_{cfrp} + L_{steel}*(CTE_{cfrp}-CTE_{steel})/L_{rod}$$

The CTE of the CFRP itself is taken as 0.3 x10^{-6} /°C. Table 1 (see & 1.3) shows the equivalent CTE for each family of strut ranging from 1.94 (rod WX) to 7.01 x10^{-6} /°C (rod BB). This arrangement leads to a smooth variation of the CTEs as a function of the radius for the circumferential struts, then only a central annulus made out of steel can fit at the center of the dish (Ring AA).

The CTE of the CFRP doesn't need to be the lowest possible as the governing parameter is the length of the steel part (end-fittings + ball joints). Therefore, a CTE <0.5 x10^{-6} /°C is tolerated for the CFRP part of the struts.

The boundary conditions are the same as for the static cases.

The following loadcases are applied separately to the reflector. Each case is qualitatively representative of a possible thermal situation.

th1 : a uniform increase of 20°C above the ambient in the whole structure.
The ambient temperature is referred to as the temperature with zero deformation. A temperature lower than the ambient would have the same effect on the surface accuracy, while the focus error and the difference in path length would be opposite in sign.

th2 : a 2°C uniform increase in the ring and the hub.

th7 : a 2°C uniform increase in the ring alone.

th4 : a 2°C linear gradient across the reflector (along y-axis), i.e. over a length of 6.1534 m or 0.325°C/m.

th5 : a 2°C linear gradient along the boresight axis (z) from the bottom of the ring to the top of the reflector, over a length of 2.364m or 0.846°C/m. This gradient does not apply to the quadrupod spars nor to M2.

th3 : a uniform increase of 2°C for the surface nodes of the BUS, i.e. the ball-joints supporting the surface panels

th6 : a uniform increase of 2°C in the quadrupod spars and M2

The following table gives for each loadcase, the surface accuracy deterioration, the pointing error, the focus error and the path length error.

	Surface accuracy (µm rms)	pointing error (arc sec.)	Focus error (µm)	Path length error (µm)	LC Nr.
Th1 20°C all BUS+ring	3.1	0.8	180	101	8
Th2 2°C ring+hub	2.9	0.1	-57	-5	9
Th7 2°C in ring	0.6	0.0	4	1	14
Th4 2°C y-lin grad	.04	0.7	0	0	11
Th5 2°C z-lin grad	0.6	0.1	54	5	12
Th3 2°C M1	1.0	0.0	101	16	10
Th6 2°C M2+quad	0.7	0.0	14	20	13

Appendixes 12 to 15 show the magnified deformed structure for the 7 thermal loadcases, appendix 16 show the corresponding residual deviations from BFPs and app.17 show their characteristics.

4. Further improvements

The key points are :

- *Standardize the BUS struts*
- *Optimize the box-type structures : ring, hub*
- *Quadrupod, improve the pointing performance for wind loads*

It is still possible to improve the behavior of the reflector for the gravity loadcases as far as surface accuracy is concerned by optimizing the cross sections of the CFRP struts of the back-up structure, but the main interest is to reduce the number of families of struts.

It will also be possible to reduce the pointing error due to the wind acting on the spars by modeling more accurately the loads on the spars and the secondary support. This secondary mirror support assembly and spars is indeed more sensitive to wind loads since we have to find the optimum rigidity for the spars in order to minimize the blockage.

Finally, in order to reduce the global weight of the reflector, it would be worthwhile to optimize the design of the box-type structures (hub and ring).

References

[1] J.Delannoy, "Least Squares fit for axisymmetric paraboloids", IRAM Internal report Nr.12, 1980
[2] S. von Hoerner, "The design and improvements of Tiltable Radio-Telescopes", 1987

FIG. 1

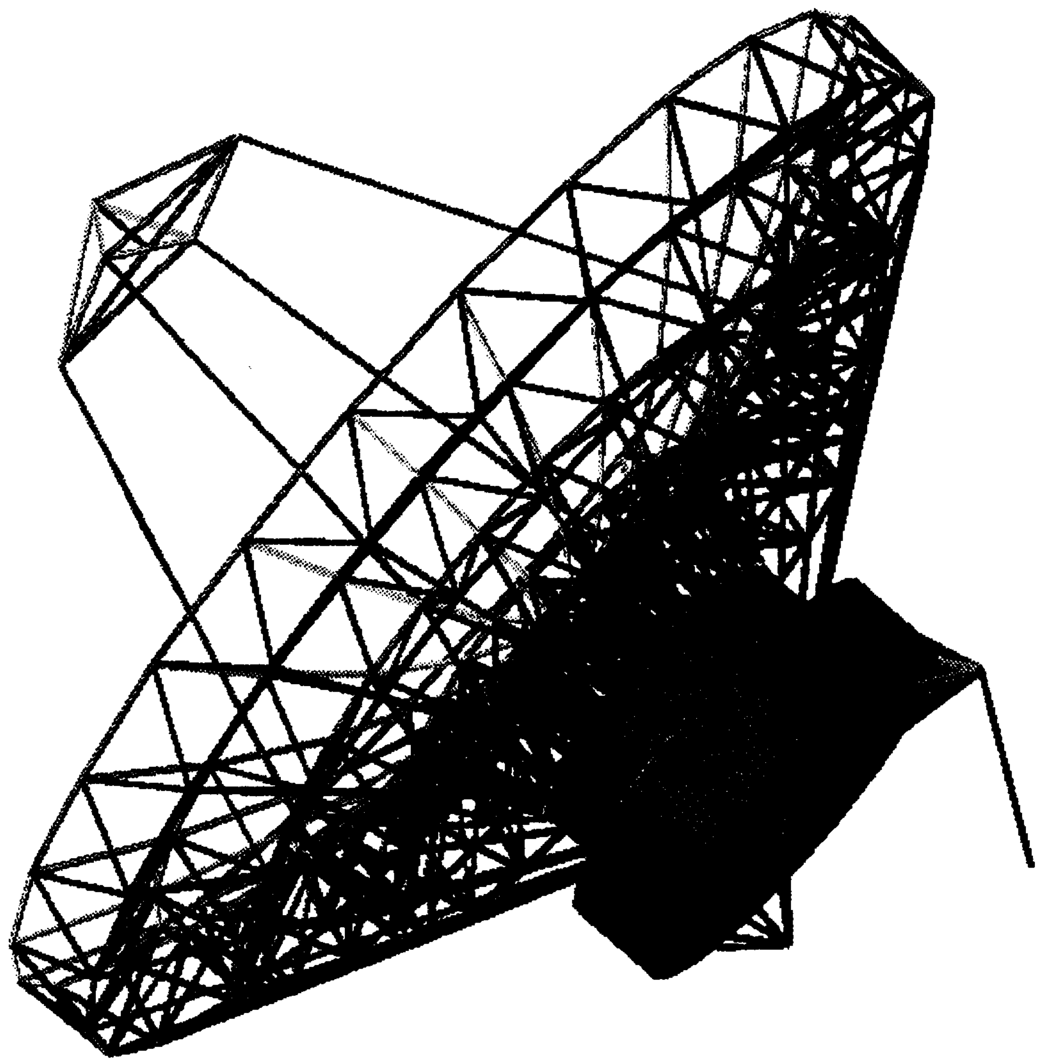

VIEW OF THE REFLECTOR AT El = 50°

Fig. 2

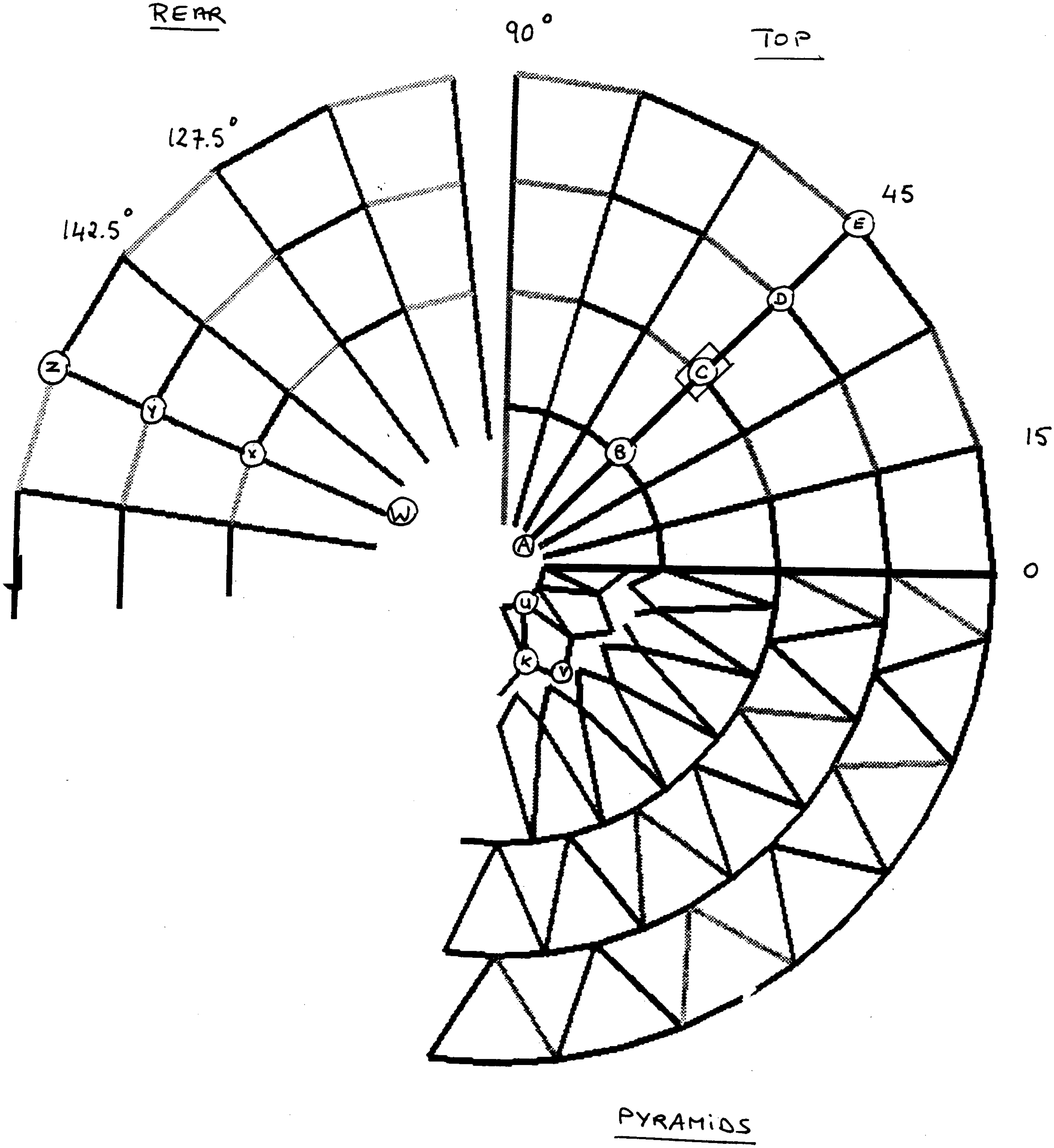

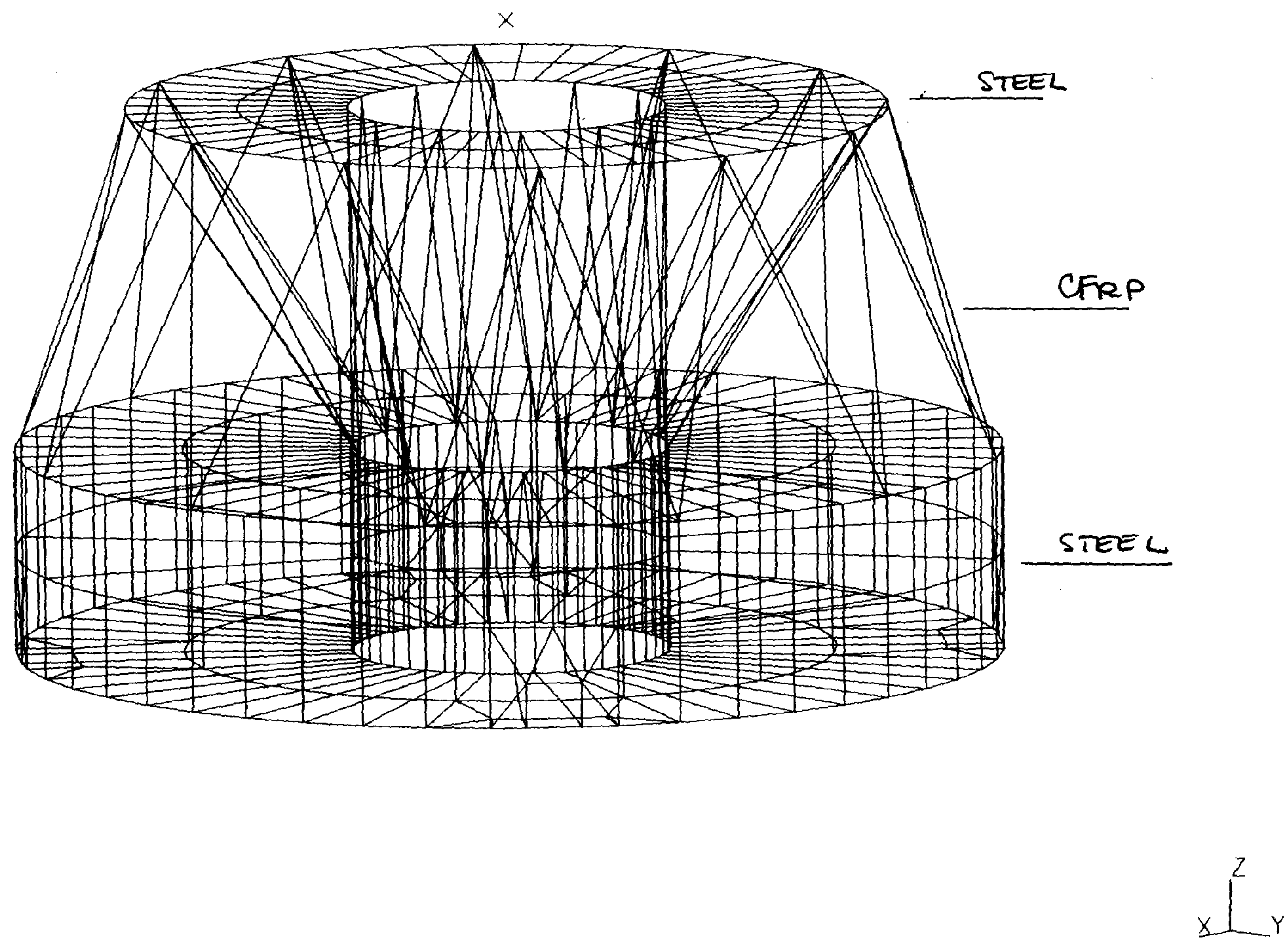

THE HUB

THE RING

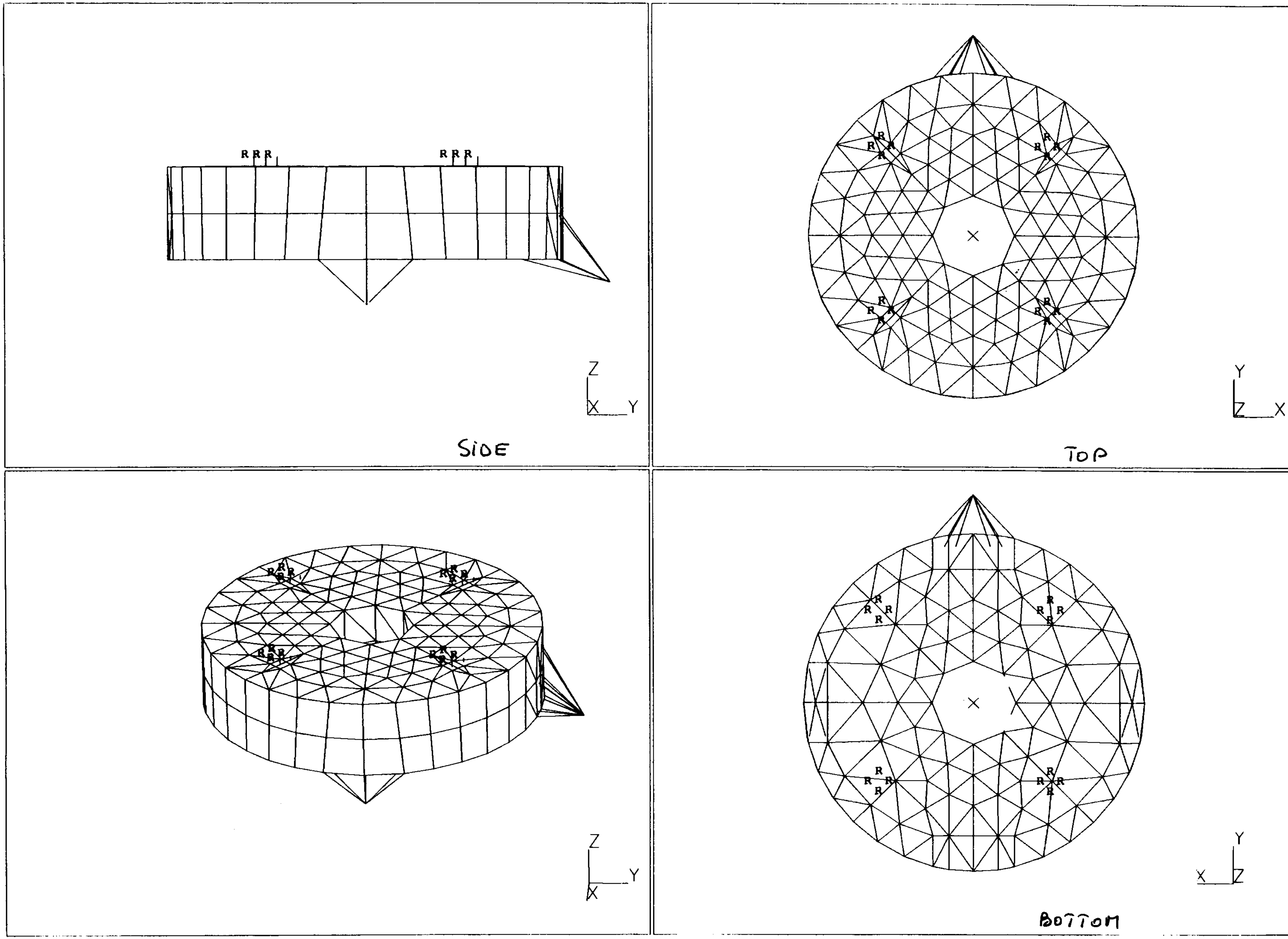

<u>THE RING</u>

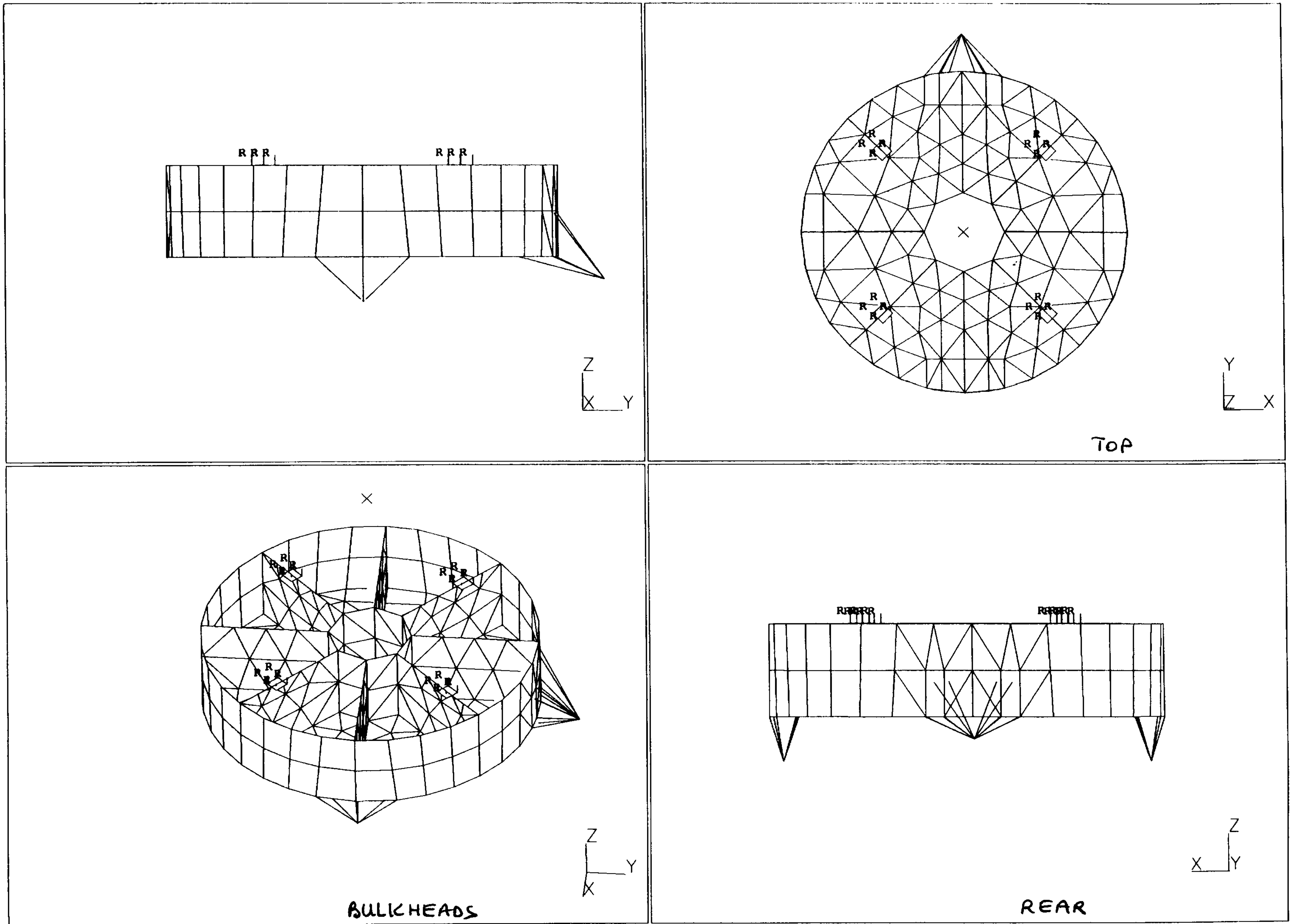

Fig. 5

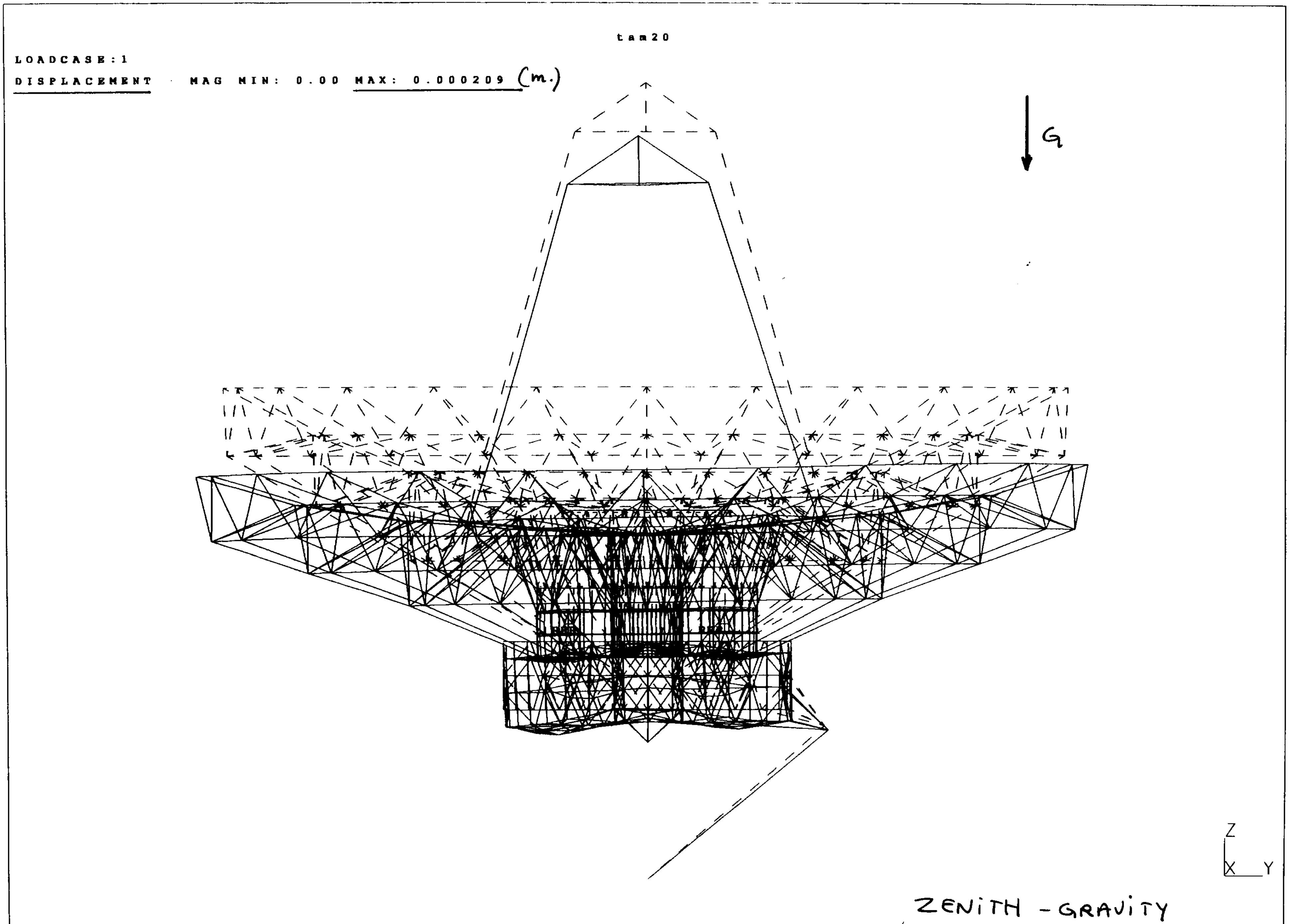

ZENITH - GRAVITY

App-1

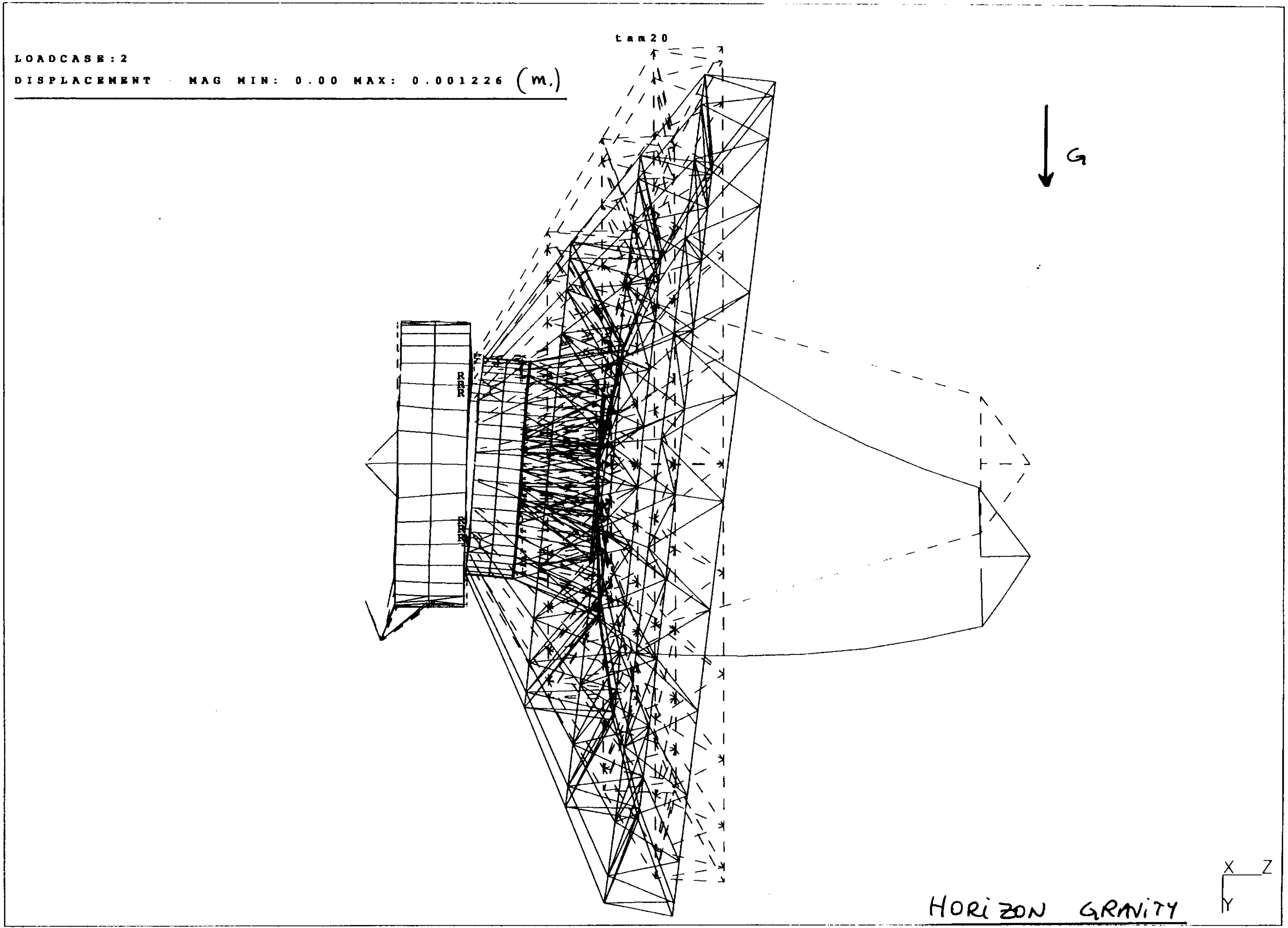
LOADCASE:2
DISPLACEMENT MAG MIN: 0.00 MAX: 0.001226 (m.)
tam20
G
HORIZON GRAVITY
X
Z
Y

App. 2

RESIDUAL DEVIATIONS FROM BEST FIT PARABOLOID

MODEL TAM20 /29−SEPT−1991/PhR/ GRAVITY LOADCASES

ZENITH

$\sigma=4.3\mu m$ r.m.s.

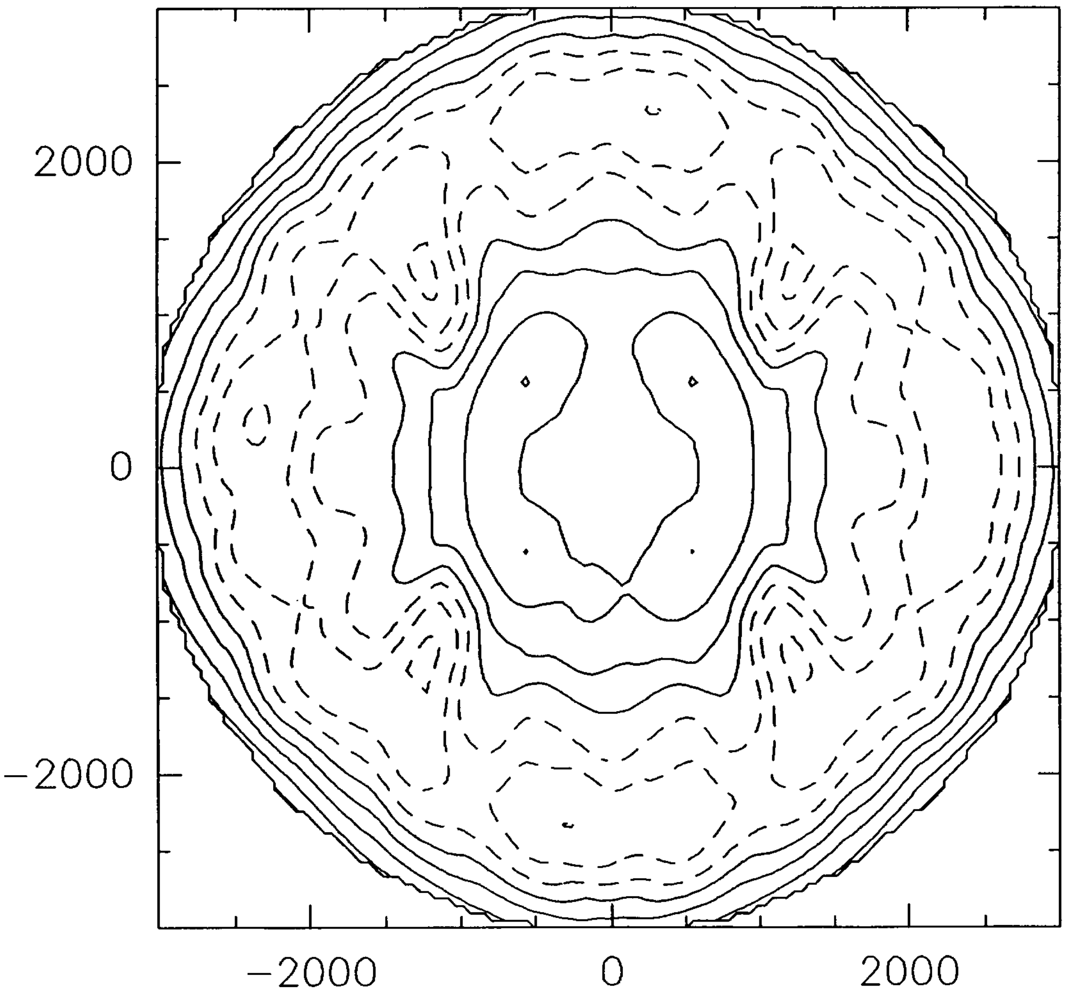

LEVELS −6 TO 8.5 BY 2 μm

HORIZON

$\sigma=6.7\mu m$ r.m.s.

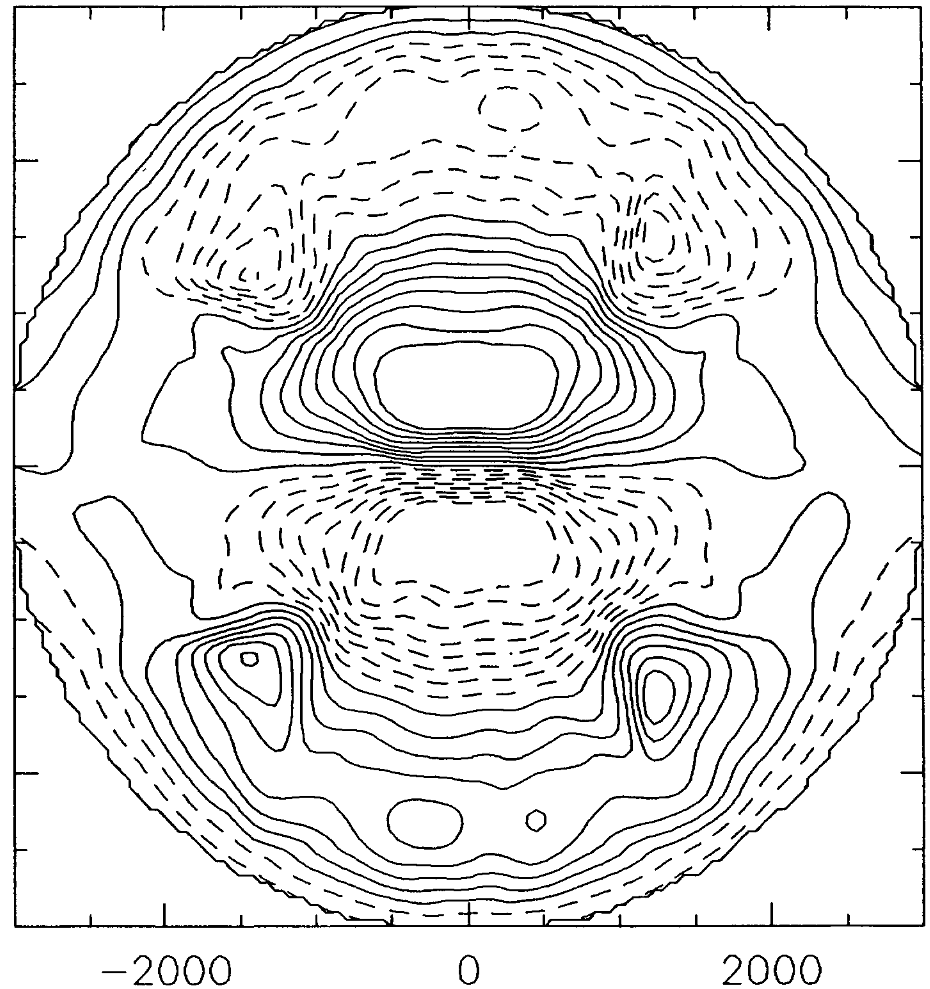

LEVELS −16 TO 16 BY 2 μm

App. 3

SMA-6M * gravity zenith (TAM20/20.Sept.91/PhR)

NEW FOCAL LENGTH (MM) =	2520.460475					
VERTEX DISP.(MM)	DX=	0.000	DY=	-0.005	DZ=	-0.052
FOCUS DISP.(MM)	DX=	0.000	DY=	-0.015	DZ=	0.408
CENTER OF CURVATURE DISP.(MM)	DX=	0.000	DY=	-0.026	DZ=	0.869
SURFACE ERROR =	4.251 MICROMETERS R.M.S.					

	(dV-dF)/f	Kp(dS-dF)/f	-(Ks/M).dS/f	-(2c/f).Ks.Y/M	TOTAL
(ARC SEC)	0.9	0.0	0.1	-0.1	0.8
Rotation about El-axis					0.9

M1 mean disp (x,y,z) =	0.000	-0.006	-0.123
M2 mean disp (x,y,z) =	0.000	-0.016	-0.121

Focus Err= 0.339 Phase Err = 0.031

SMA-6M * GRAV. Ho (TAM20/20.Sept.91/PhR)

NEW FOCAL LENGTH (MM) =	2520.000183					
VERTEX DISP.(MM)	DX=	0.000	DY=	-1.824	DZ=	0.002
FOCUS DISP.(MM)	DX=	0.000	DY=	-0.383	DZ=	0.003
CENTER OF CURVATURE DISP.(MM)	DX=	0.000	DY=	1.057	DZ=	0.003
SURFACE ERROR =	6.670 MICROMETERS R.M.S.					

	(dV-dF)/f	Kp(dS-dF)/f	-(Ks/M).dS/f	-(2c/f).Ks.Y/M	TOTAL
(ARC SEC)	-117.9	109.7	-4.2	-0.7	-13.2
Rotation about El-axis					-2.6

M1 mean disp (x,y,z) =	0.000	0.340	0.002
M2 mean disp (x,y,z) =	0.000	1.232	0.002

Focus Err= 0.003 Phase Err = 0.000

WiND El=0

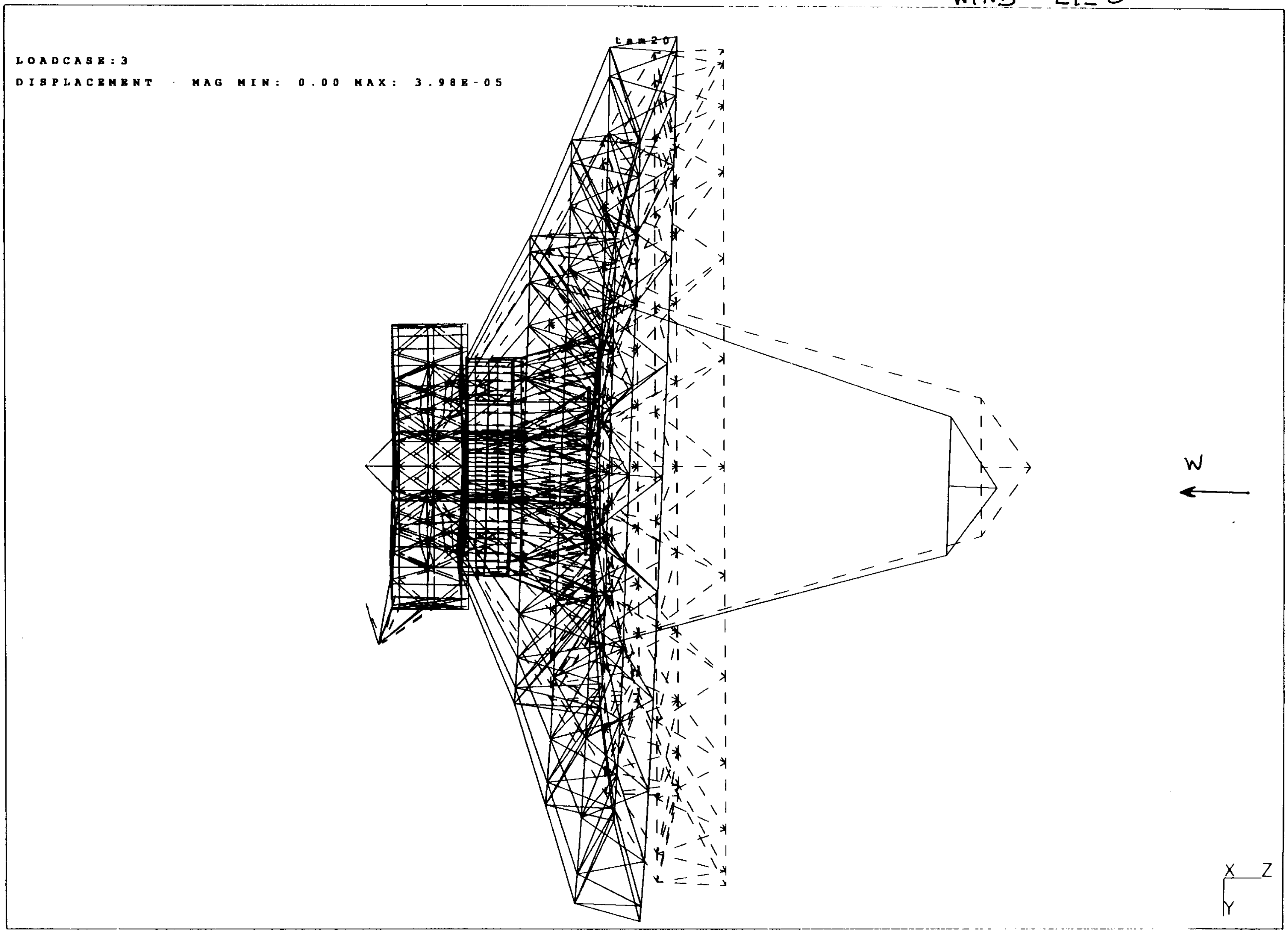

App. 5

WIND EL= 30

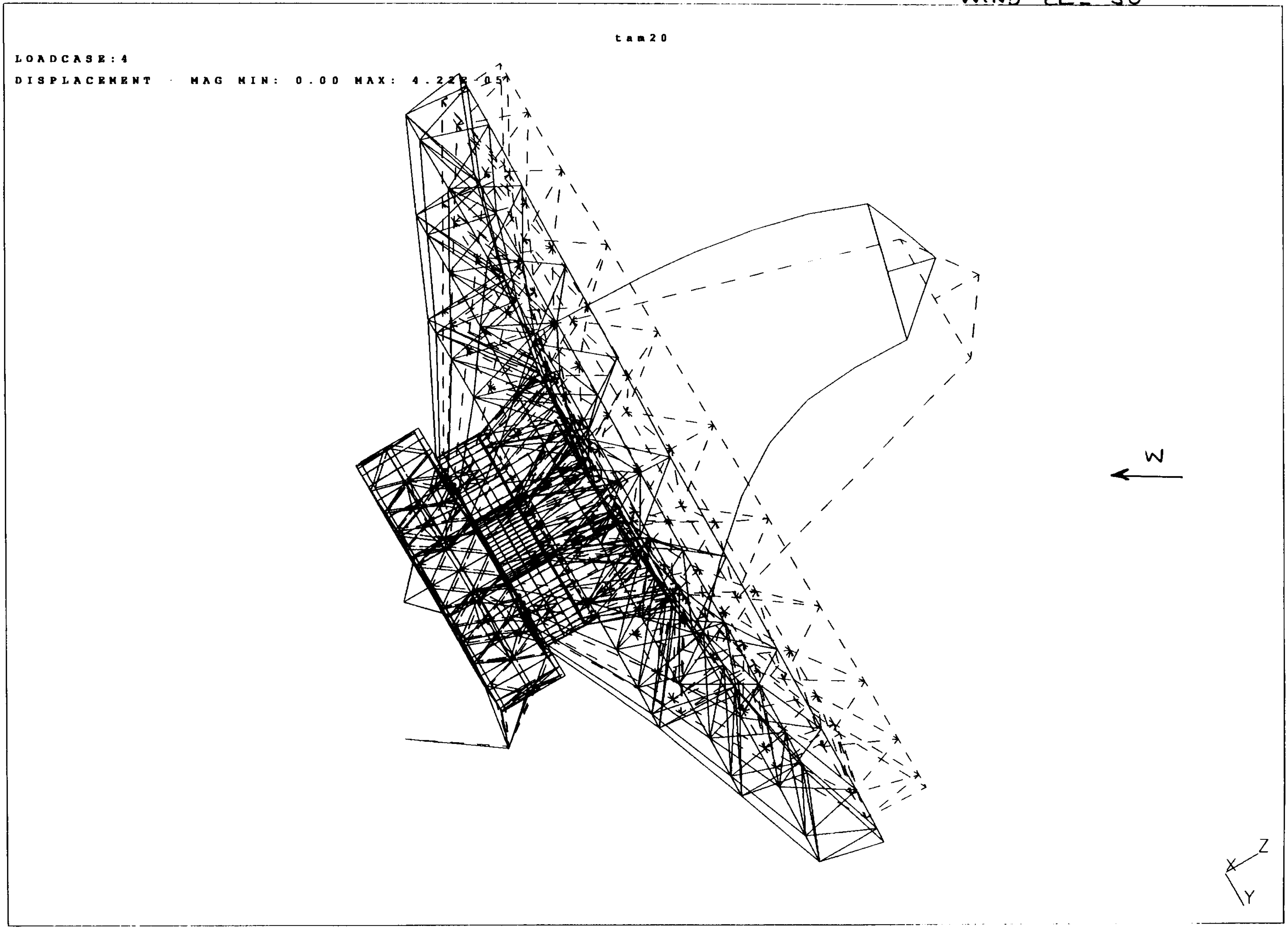

App. 6

WIND EL= 50

tam20

LOADCASE:5

DISPLACEMENT - MAG MIN: 0.00 MAX: 7.25E-05

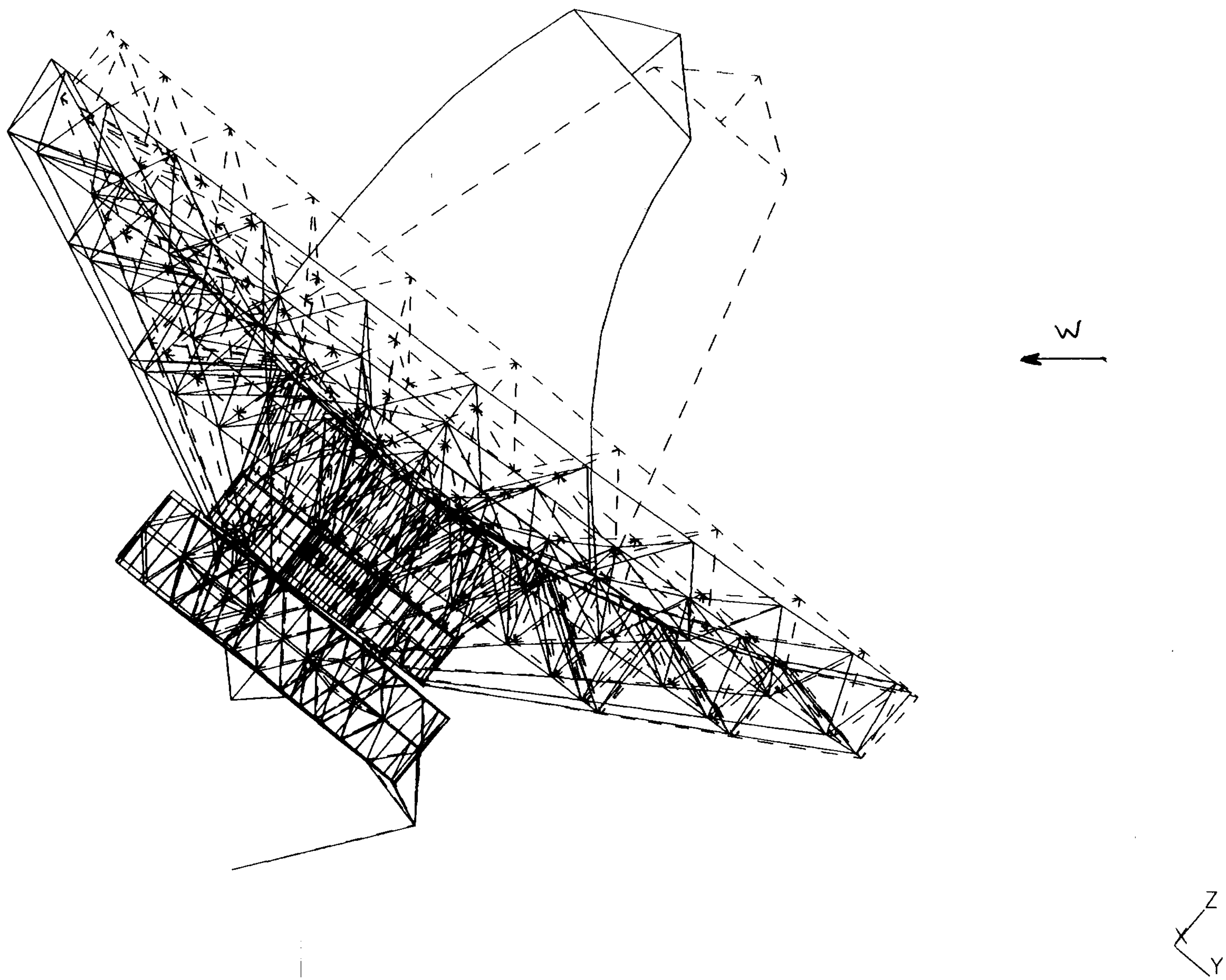

App. 7

WIND EL= 70

tam20

LOADCASE:6

DISPLACEMENT - MAG MIN: 0.00 MAX: 8.03E-05

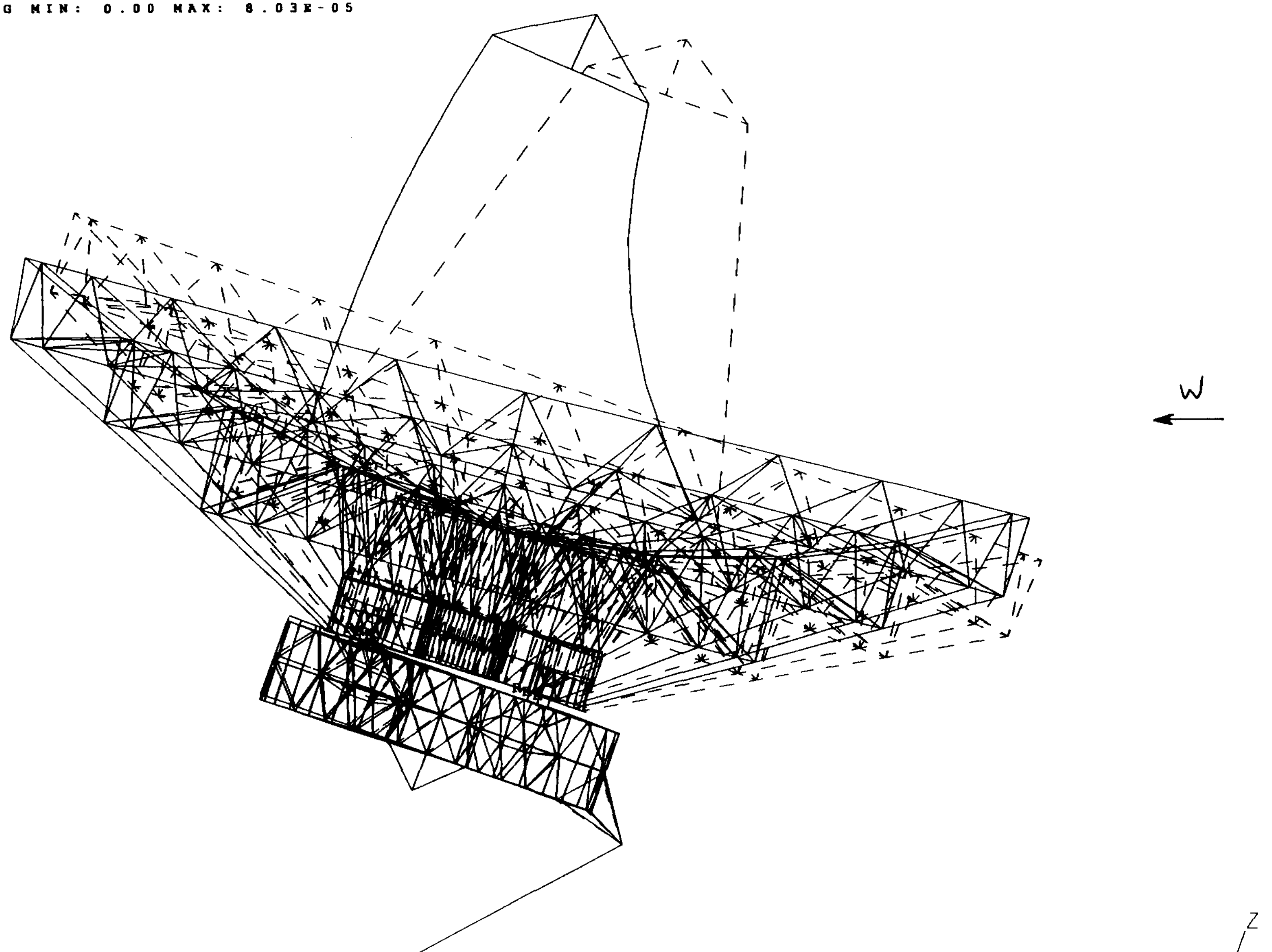

App. 8

WIND EL = 90

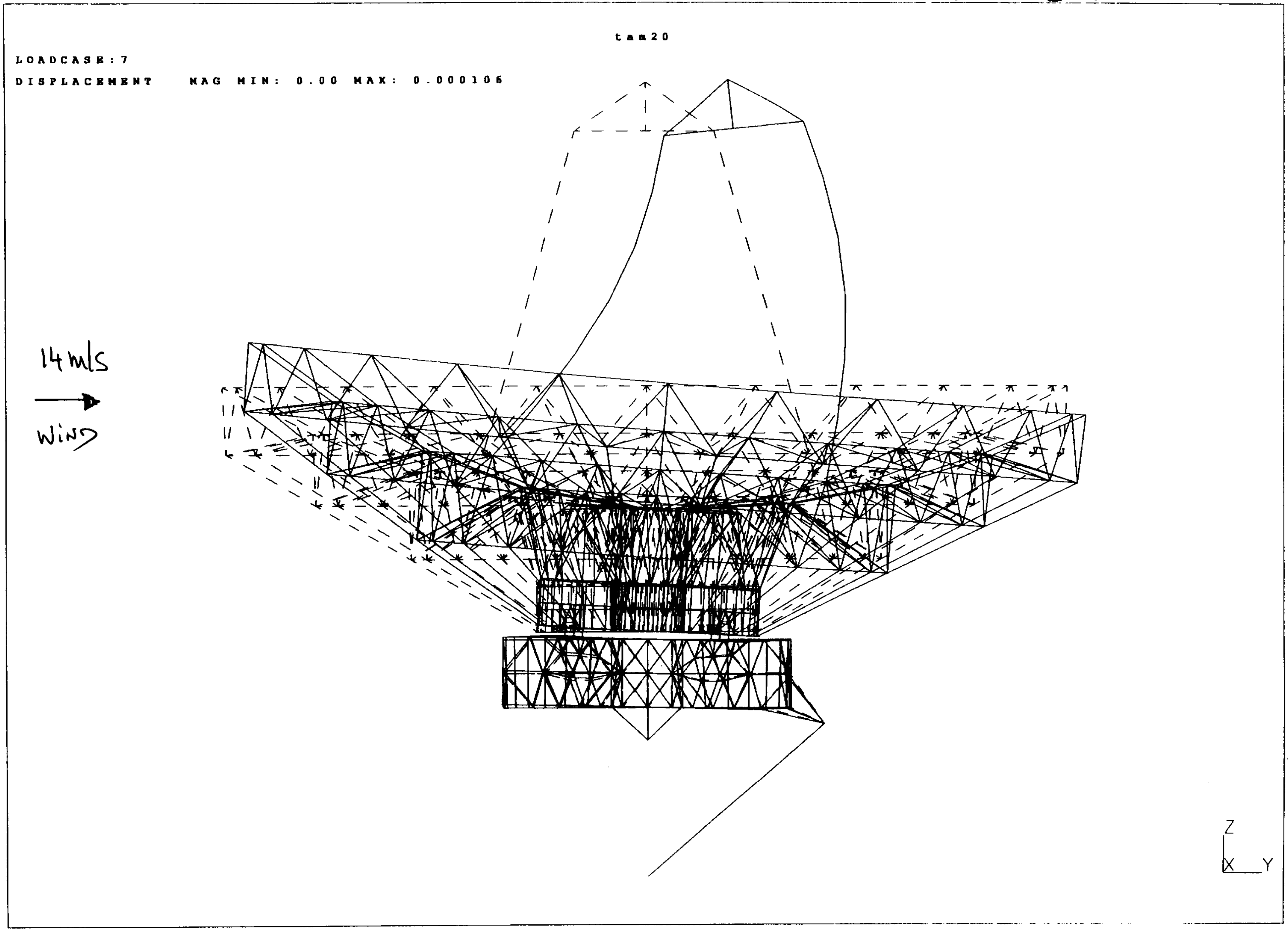

App. 9

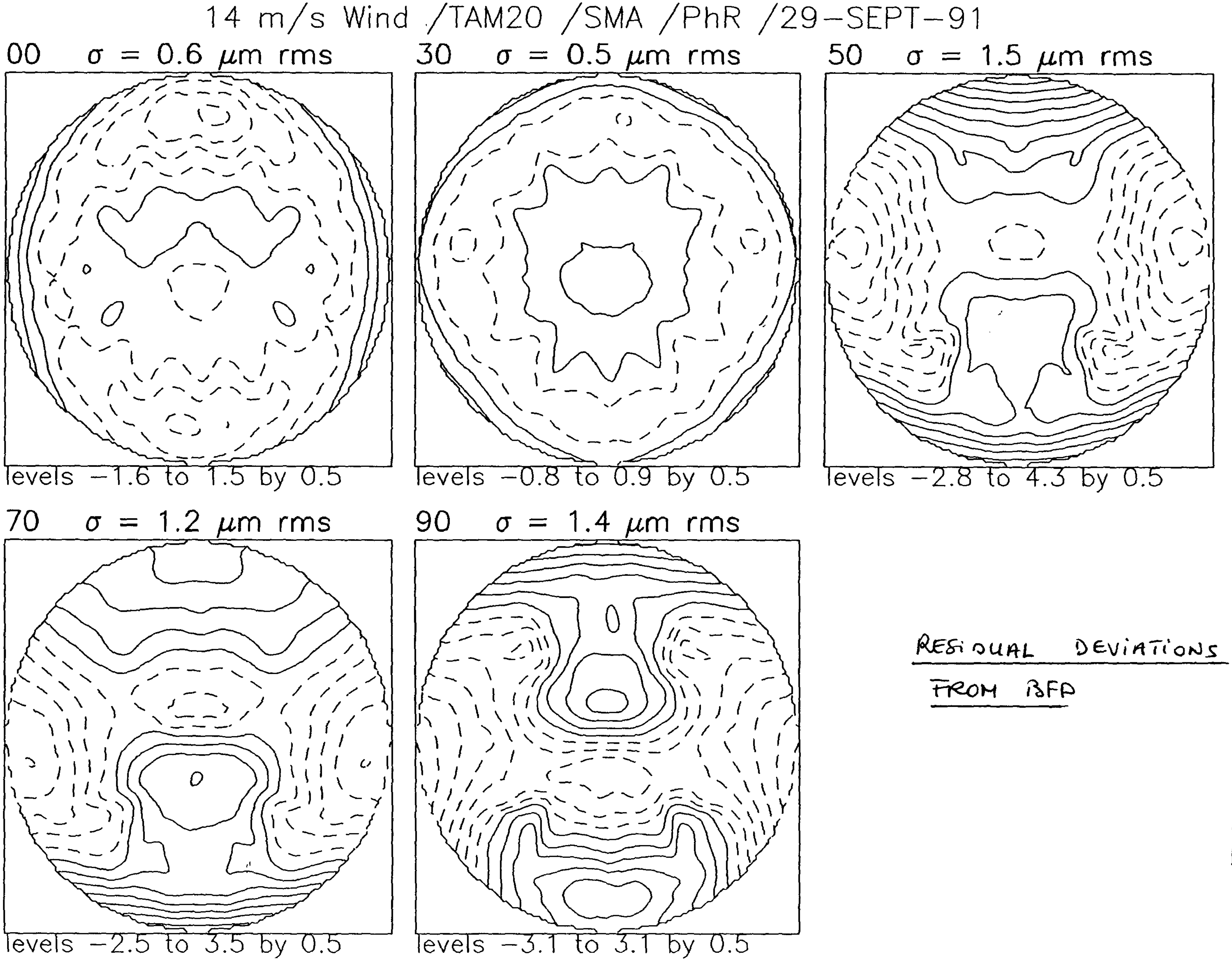
14 m/s Wind /TAM20 /SMA /PhR /29-SEPT-91
00 σ = 0.6 μm rms
levels −1.6 to 1.5 by 0.5
30 σ = 0.5 μm rms
levels −0.8 to 0.9 by 0.5
50 σ = 1.5 μm rms
levels −2.8 to 4.3 by 0.5
70 σ = 1.2 μm rms
levels −2.5 to 3.5 by 0.5
90 σ = 1.4 μm rms
levels −3.1 to 3.1 by 0.5
RESIDUAL DEVIATIONS
FROM BFP

App. 10

SMA-6M * WIND 00 (TAM20/20.Sept.91/PhR)

NEW FOCAL LENGTH (MM) = 2520.080369

VERTEX DISP.(MM)	DX=	0.000	DY=	-0.026	DZ=	-0.004
FOCUS DISP.(MM)	DX=	0.000	DY=	-0.007	DZ=	0.076
CENTER OF CURVATURE DISP.(MM)	DX=	0.000	DY=	0.012	DZ=	0.157

SURFACE ERROR = 0.649 MICROMETERS R.M.S.

	(dV-dF)/f	Kp(dS-dF)/f	-(Ks/M).dS/f	-(2c/f).Ks.Y/M	TOTAL
(ARC SEC)	-1.5	1.0	0.0	0.0	-0.5
Rotation about El-axis					0.0

	x	y	z
M1 mean disp (x,y,z) =	0.000	0.003	-0.016
M2 mean disp (x,y,z) =	0.000	0.008	-0.014

Focus Err= 0.066 Phase Err = 0.010

SMA-6M * WIND 30 (TAM20/23.Sept.91/PhR)

NEW FOCAL LENGTH (MM) = 2520.069847

VERTEX DISP.(MM)	DX=	0.000	DY=	-0.033	DZ=	-0.004
FOCUS DISP.(MM)	DX=	0.000	DY=	-0.014	DZ=	0.066
CENTER OF CURVATURE DISP.(MM)	DX=	0.000	DY=	0.006	DZ=	0.136

SURFACE ERROR = 0.472 MICROMETERS R.M.S.

	(dV-dF)/f	Kp(dS-dF)/f	-(Ks/M).dS/f	-(2c/f).Ks.Y/M	TOTAL
(ARC SEC)	-1.6	-0.7	0.1	0.2	-1.9
Rotation about El-axis					0.0

	x	y	z
M1 mean disp (x,y,z) =	0.000	0.002	-0.014
M2 mean disp (x,y,z) =	0.000	-0.023	-0.013

Focus Err= 0.057 Phase Err = 0.008

SMA-6M * WIND 50 (TAM20/20.Sept.91/PhR)

NEW FOCAL LENGTH (MM) = 2520.065671

VERTEX DISP.(MM)	DX=	0.000	DY=	0.041	DZ=	-0.004
FOCUS DISP.(MM)	DX=	0.000	DY=	0.007	DZ=	0.062
CENTER OF CURVATURE DISP.(MM)	DX=	0.000	DY=	-0.028	DZ=	0.128

SURFACE ERROR = 1.458 MICROMETERS R.M.S.

	(dV-dF)/f	Kp(dS-dF)/f	-(Ks/M).dS/f	-(2c/f).Ks.Y/M	TOTAL
(ARC SEC)	2.8	-4.8	0.2	0.3	-1.5
Rotation about El-axis					0.2

	x	y	z
M1 mean disp (x,y,z) =	0.000	-0.008	-0.014
M2 mean disp (x,y,z) =	0.000	-0.063	-0.012

Focus Err= 0.053 Phase Err = 0.007

SMA-6M * WIND 70 (TAM20/20.Sept.91/PhR)

NEW FOCAL LENGTH (MM) =	2520.029635					
VERTEX DISP.(MM)	DX=	0.000	DY=	0.091	DZ=	-0.002
FOCUS DISP.(MM)	DX=	0.000	DY=	0.020	DZ=	0.028
CENTER OF CURVATURE DISP.(MM)	DX=	0.000	DY=	-0.051	DZ=	0.057
SURFACE ERROR =	1.231 MICROMETERS R.M.S.					

	(dV-dF)/f	Kp(dS-dF)/f	-(Ks/M).dS/f	-(2c/f).Ks.Y/M	TOTAL
(ARC SEC)	5.8	-6.2	0.2	0.1	0.0
Rotation about El-axis					0.2

M1 mean disp (x,y,z) =	0.000	-0.014	-0.007
M2 mean disp (x,y,z) =	0.000	-0.071	-0.006

Focus Err= 0.024 Phase Err = 0.004

SMA-6M * WIND 90 (TAM20/20.Sept.91/PhR)

NEW FOCAL LENGTH (MM) =	2519.980850					
VERTEX DISP.(MM)	DX=	0.000	DY=	-0.107	DZ=	0.001
FOCUS DISP.(MM)	DX=	0.000	DY=	-0.021	DZ=	-0.018
CENTER OF CURVATURE DISP.(MM)	DX=	0.000	DY=	0.065	DZ=	-0.038
SURFACE ERROR =	1.445 MICROMETERS R.M.S.					

	(dV-dF)/f	Kp(dS-dF)/f	-(Ks/M).dS/f	-(2c/f).Ks.Y/M	TOTAL
(ARC SEC)	-7.0	8.4	-0.4	-0.3	0.8
Rotation about El-axis					-0.2

M1 mean disp (x,y,z) =	0.000	0.018	0.004
M2 mean disp (x,y,z) =	0.000	0.103	0.003

Focus Err= -0.016 Phase Err = -0.003

TH1

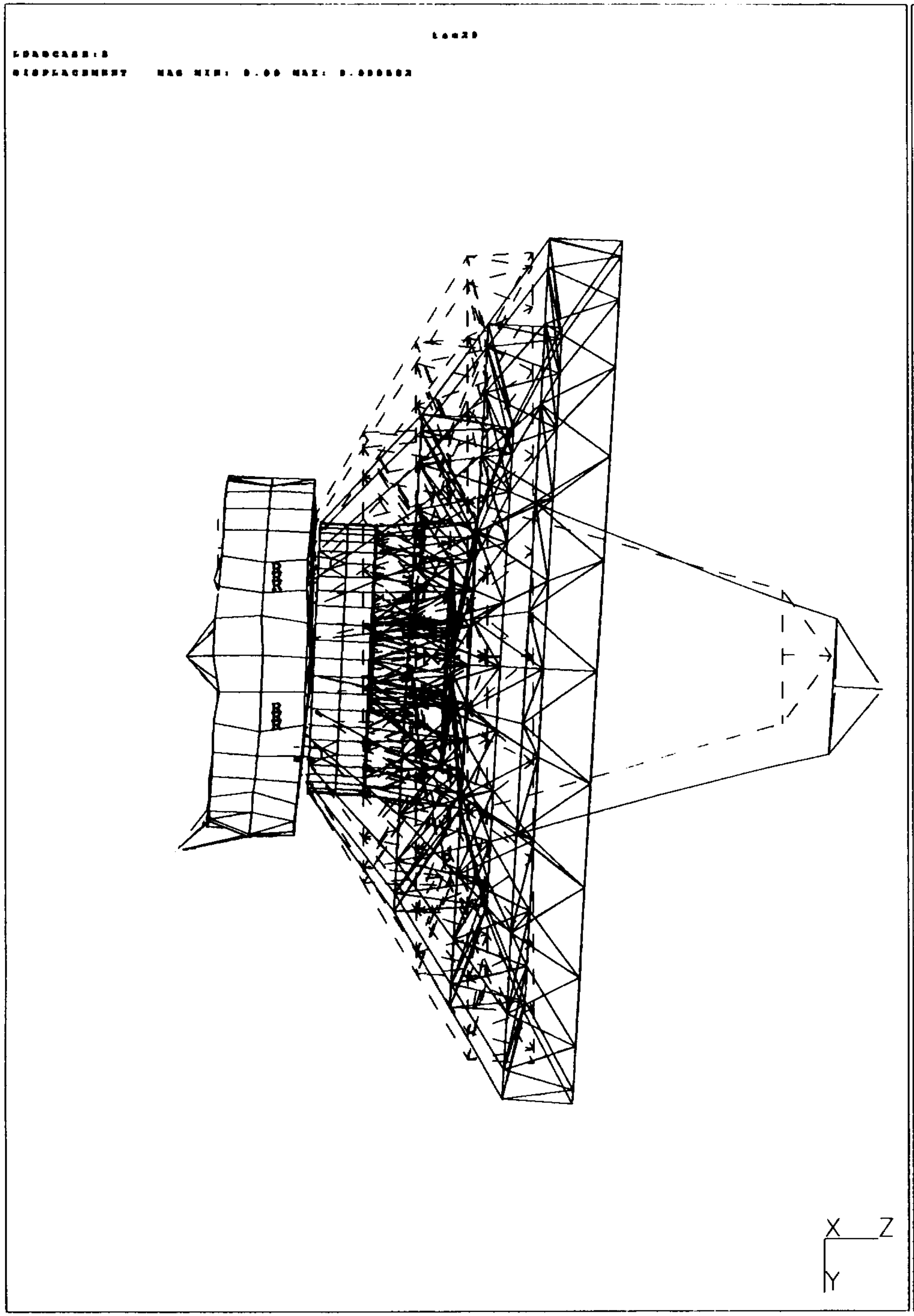

TH2

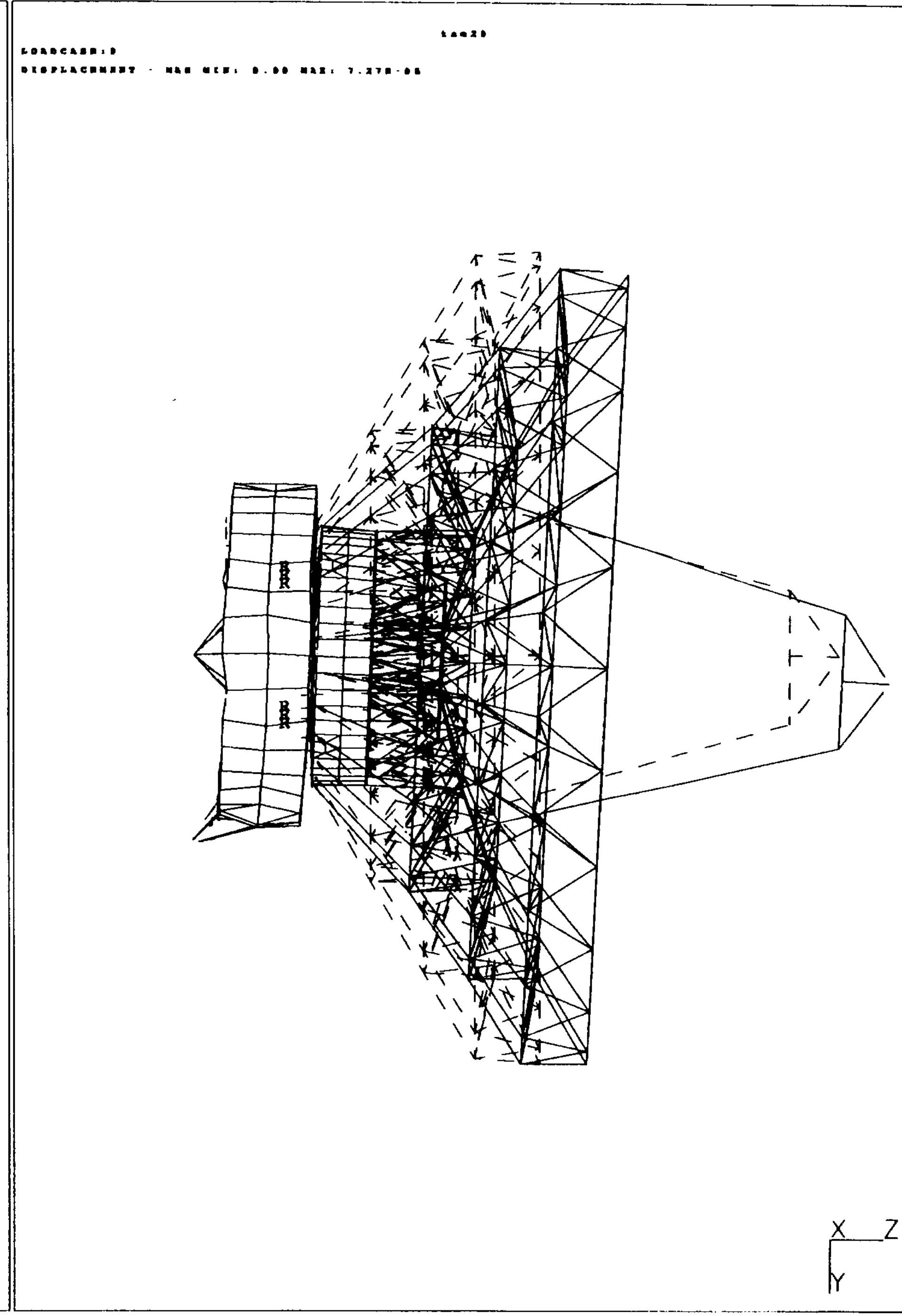

APP.1x

TH 7

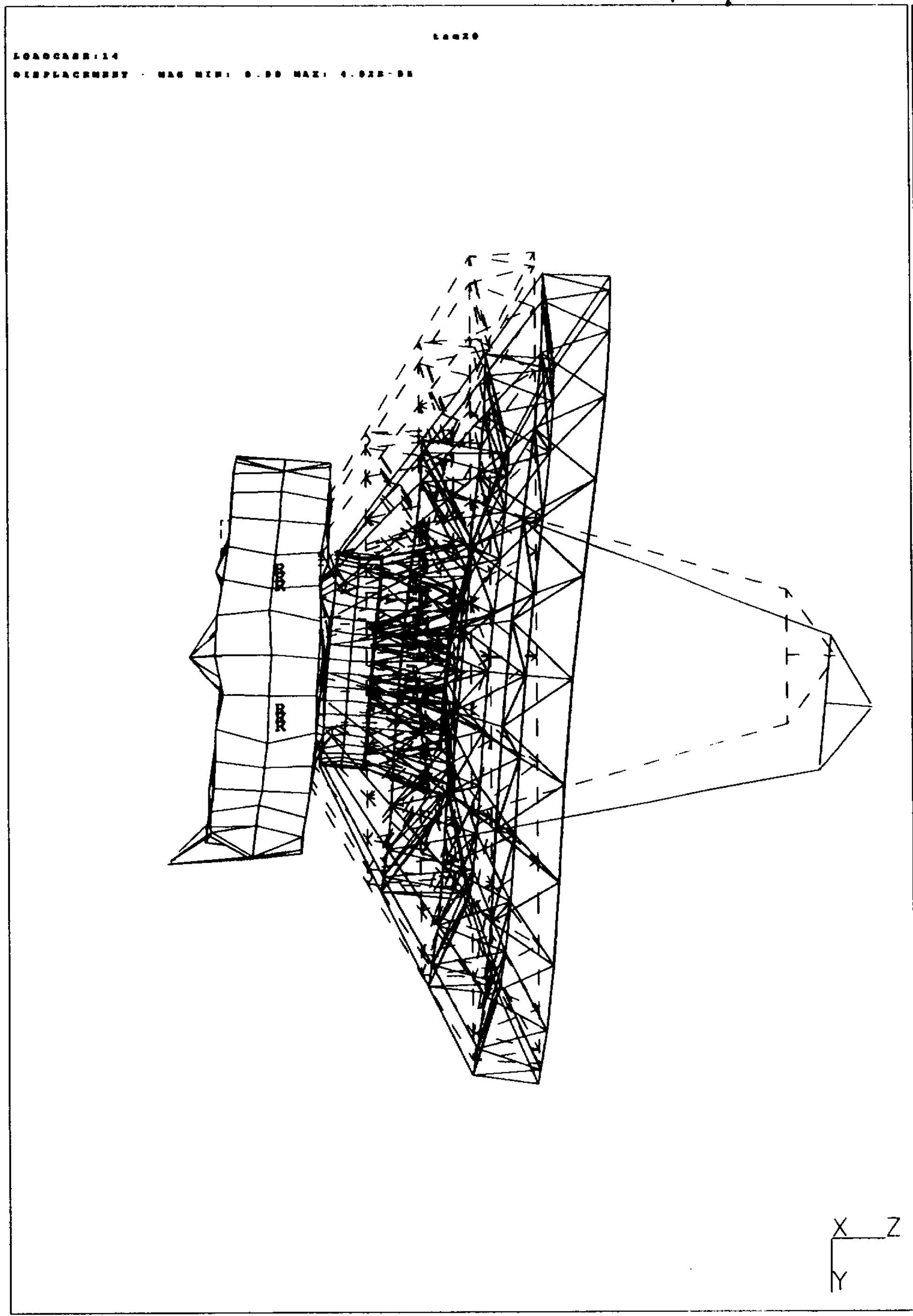

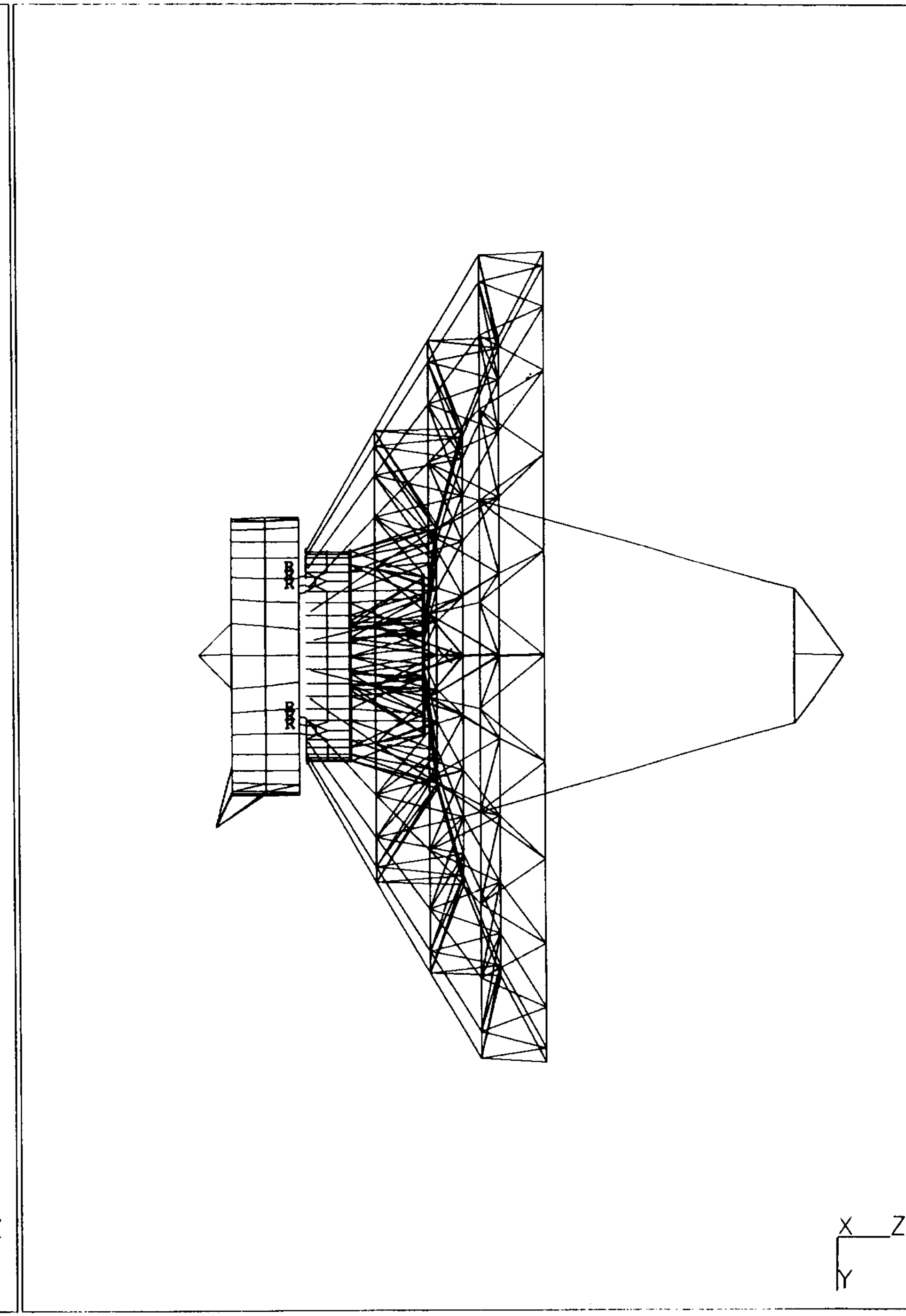

App. 13

TH4

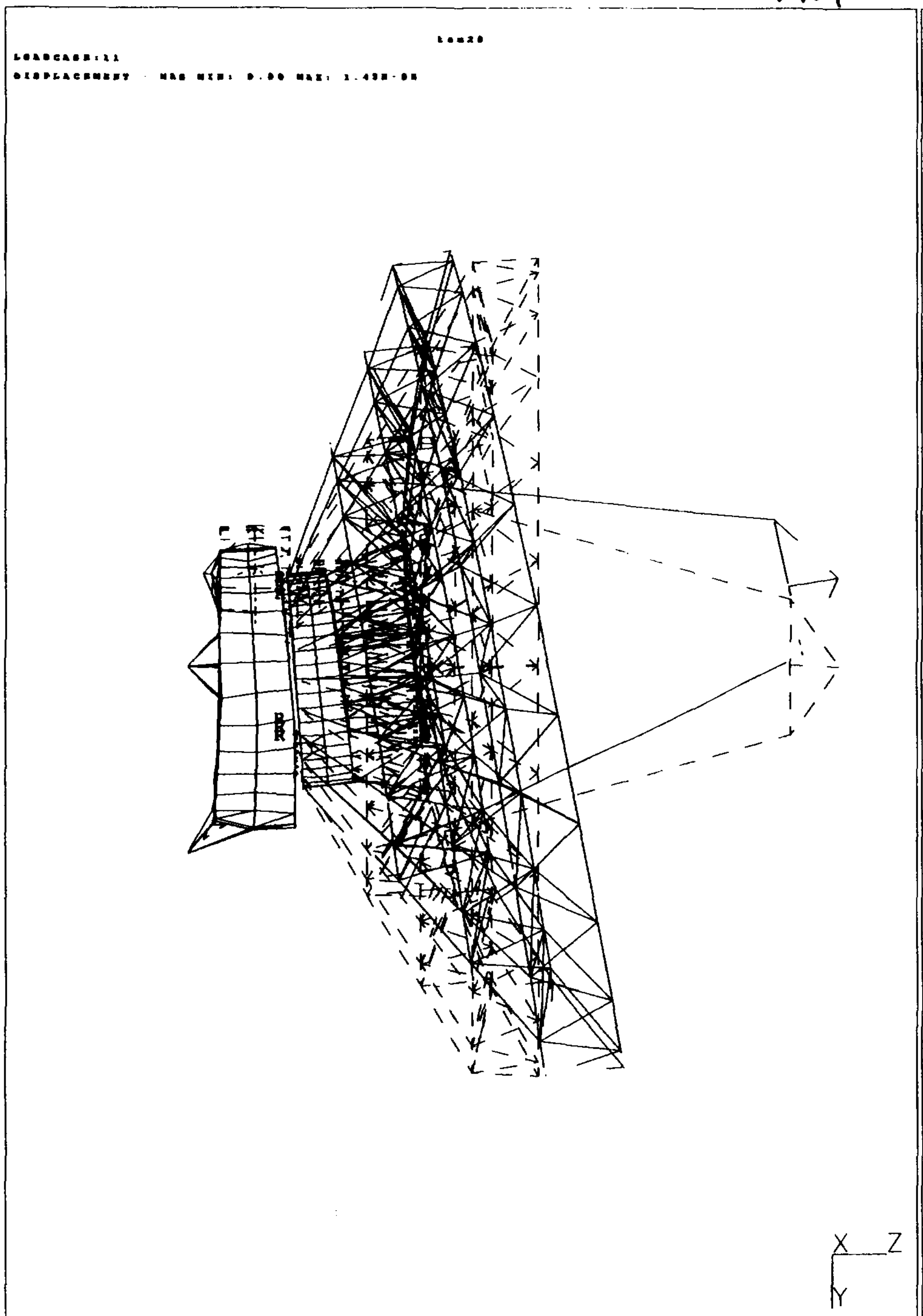

TH5

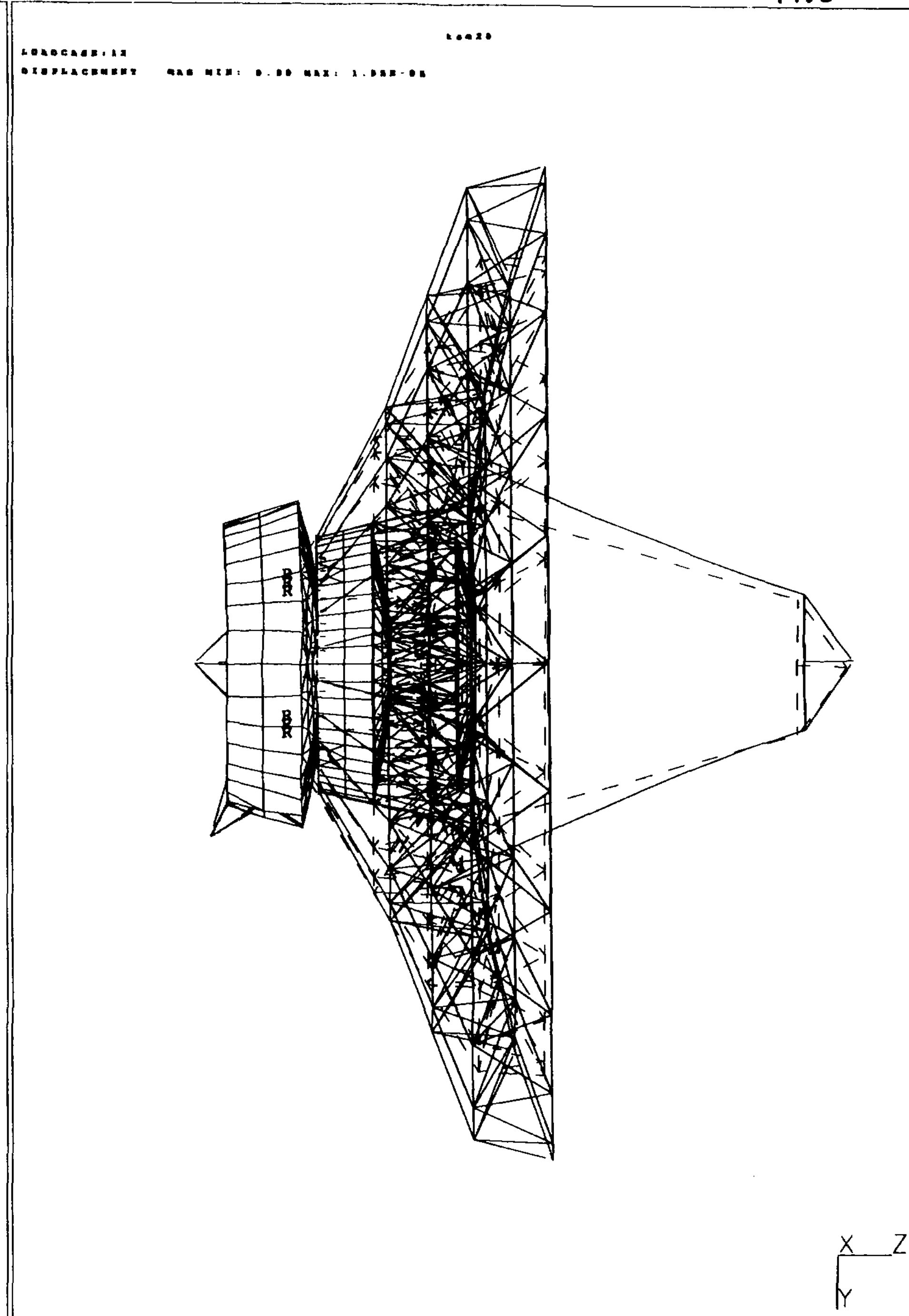

App.14

TH3

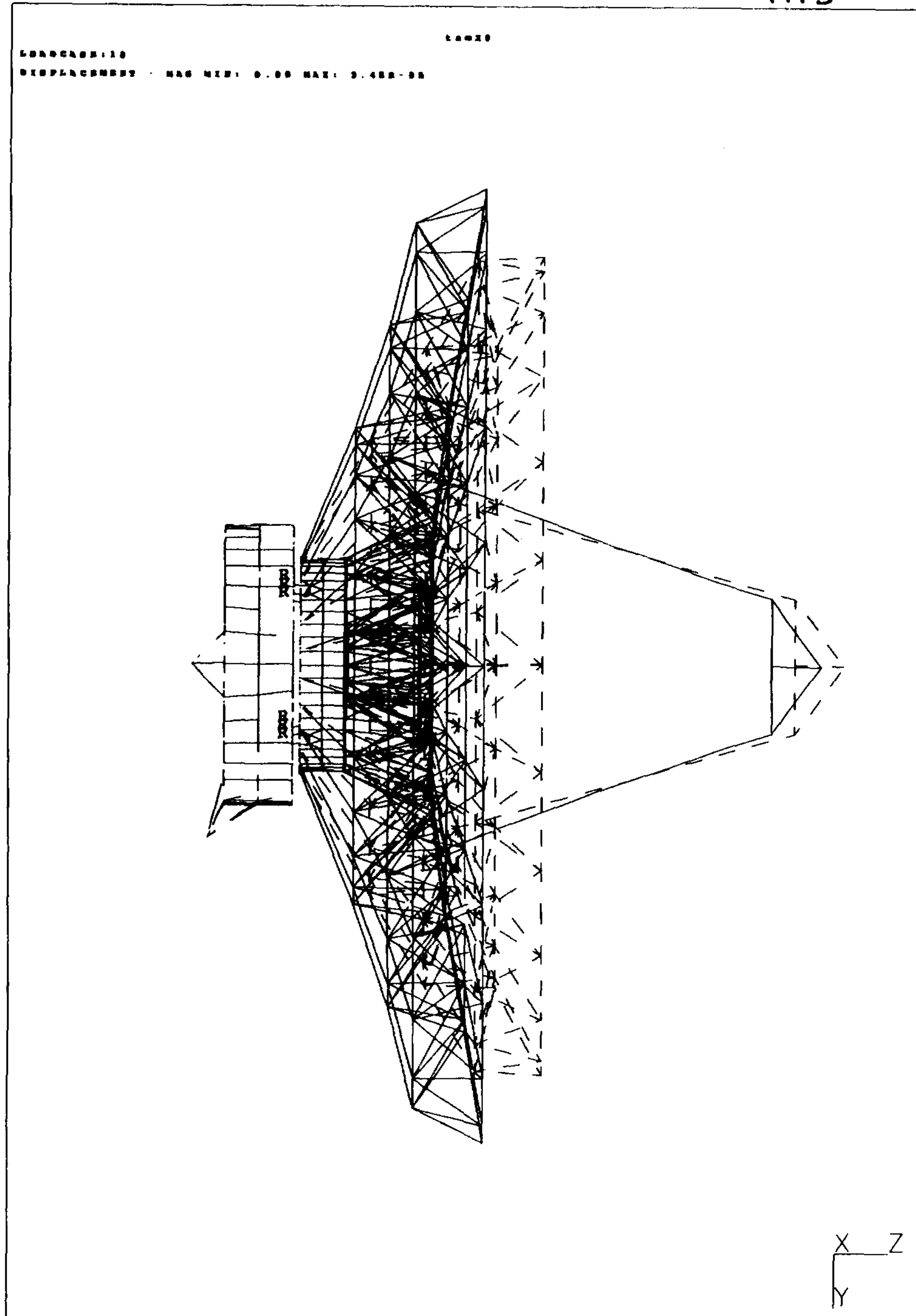

TH6

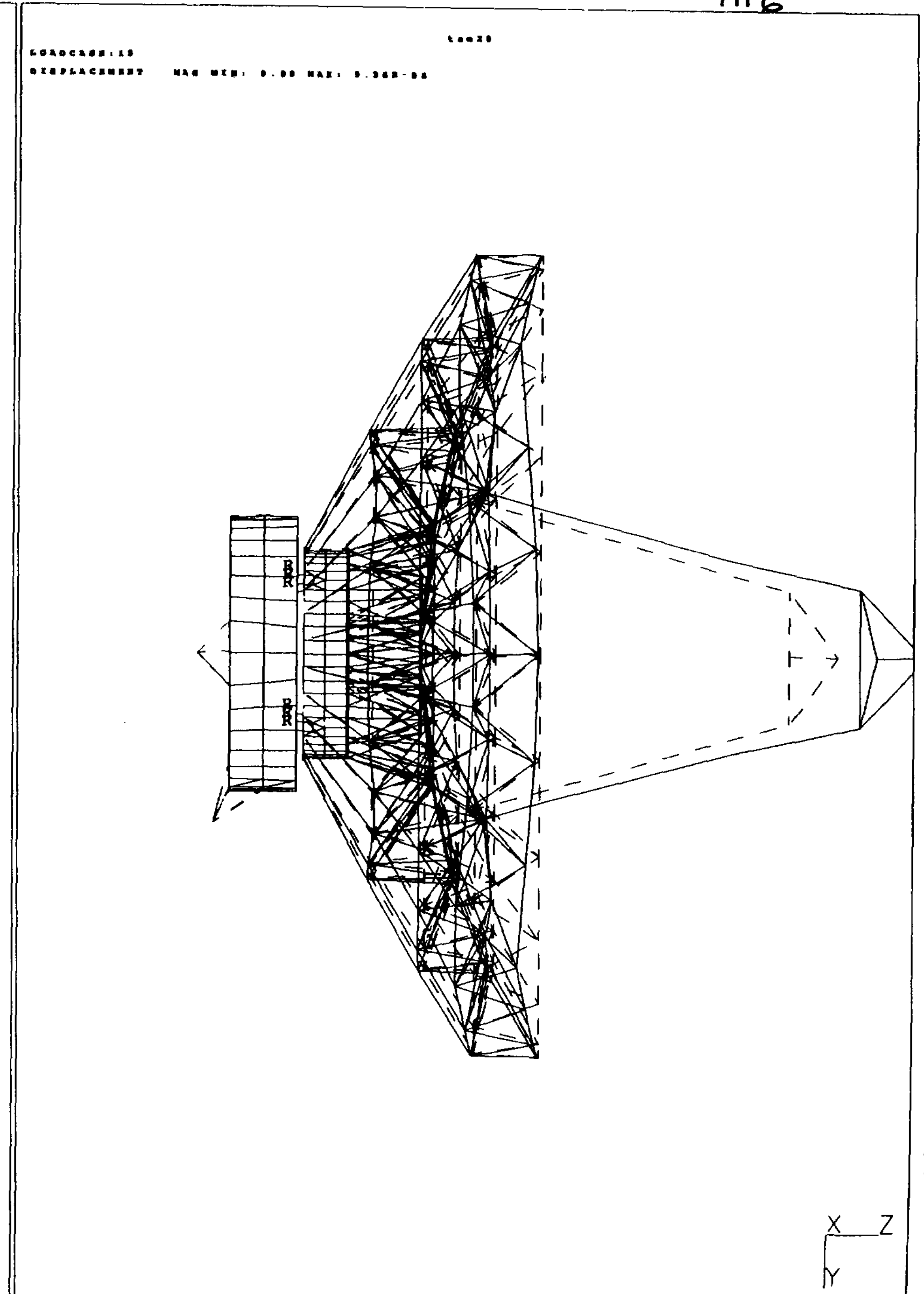

App. 15

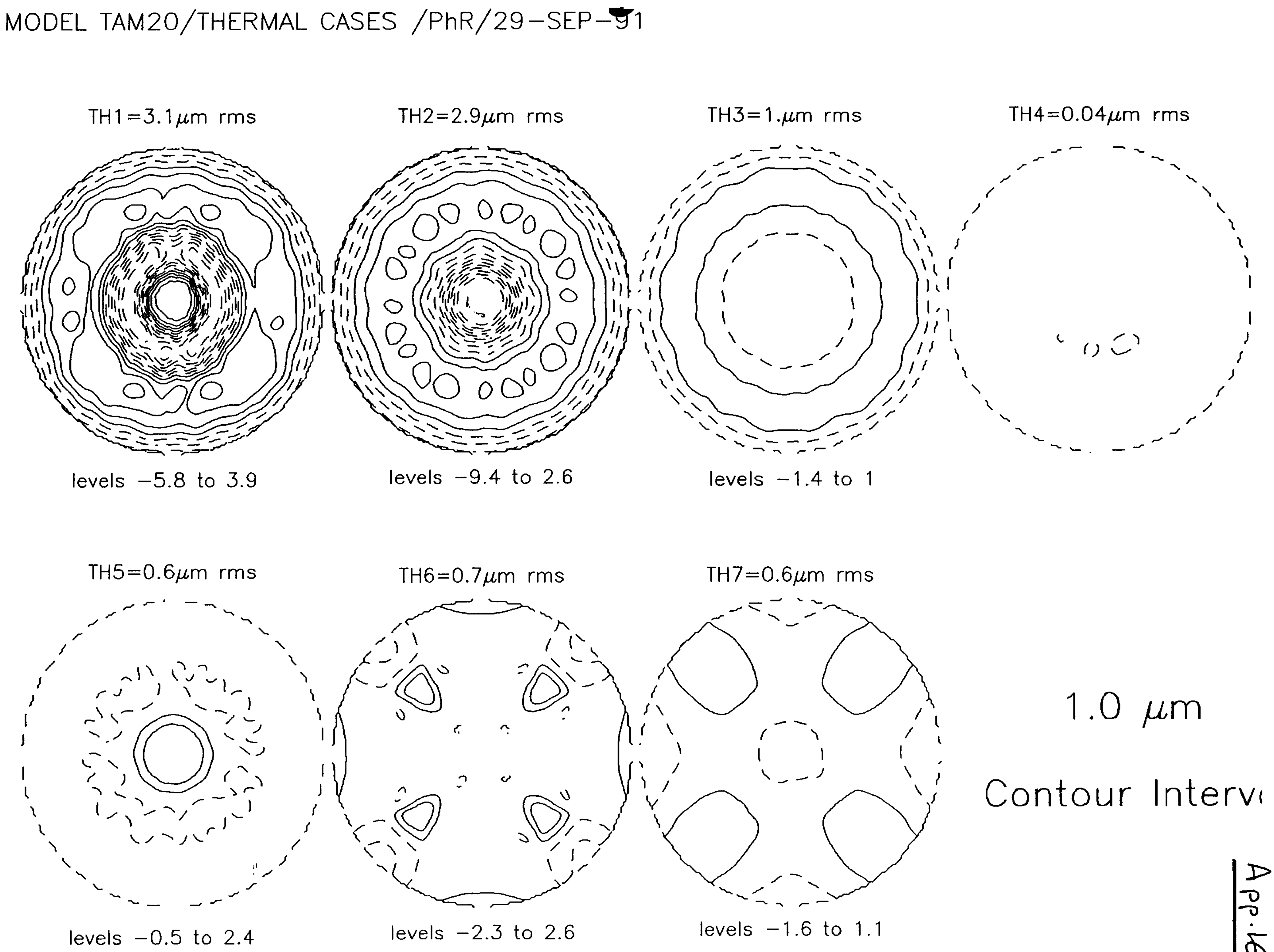
MODEL TAM20/THERMAL CASES /PhR/29-SEP-91
TH1=3.1μm rms
levels −5.8 to 3.9
TH2=2.9μm rms
levels −9.4 to 2.6
TH3=1.μm rms
levels −1.4 to 1
TH4=0.04μm rms
TH5=0.6μm rms
levels −0.5 to 2.4
TH6=0.7μm rms
levels −2.3 to 2.6
TH7=0.6μm rms
levels −1.6 to 1.1
1.0 μm
Contour Interv

```
-----------------------------------------------------------------------------
              SMA-6M * TH1 20C GLOBAL (TAM20/20.Sept.91/PhR)
-----------------------------------------------------------------------------
   NEW FOCAL LENGTH (MM)          =             2519.843712
   VERTEX DISP.(MM)                    DX= -0.003   DY=  0.052   DZ=  0.257
   FOCUS  DISP.(MM)                    DX= -0.003   DY=  0.184   DZ=  0.101
   CENTER OF CURVATURE DISP.(MM)       DX= -0.003   DY=  0.315   DZ= -0.055
   SURFACE ERROR =                       3.144  MICROMETERS R.M.S.
-----------------------------------------------------------------------------
           (dV-dF)/f  Kp(dS-dF)/f   -(Ks/M).dS/f  -(2c/f).Ks.Y/M  TOTAL
(ARC SEC)    -10.8        0.5          -0.7           0.9         -10.1
Rotation about El-axis                                            -10.9
M1 mean disp (x,y,z) =     -0.001    0.074     0.345
M2 mean disp (x,y,z) =     -0.002    0.191     0.337
Focus Err=      0.180  Phase Err =     0.101
-----------------------------------------------------------------------------
              SMA-6M * TH2 2C LOW HUB+RING (TAM20/20.Sept.91/PhR)
-----------------------------------------------------------------------------
   NEW FOCAL LENGTH (MM)          =             2519.901683
   VERTEX DISP.(MM)                    DX=  0.000   DY=  0.005   DZ=  0.026
   FOCUS  DISP.(MM)                    DX=  0.000   DY=  0.018   DZ= -0.072
   CENTER OF CURVATURE DISP.(MM)       DX=  0.000   DY=  0.032   DZ= -0.170
   SURFACE ERROR =                       2.868  MICROMETERS R.M.S.
-----------------------------------------------------------------------------
           (dV-dF)/f  Kp(dS-dF)/f   -(Ks/M).dS/f  -(2c/f).Ks.Y/M  TOTAL
(ARC SEC)     -1.1        0.0          -0.1           0.1          -1.0
Rotation about El-axis                                             -1.1
M1 mean disp (x,y,z) =      0.000    0.007     0.041
M2 mean disp (x,y,z) =      0.000    0.019     0.041
Focus Err=     -0.057  Phase Err =    -0.005
-----------------------------------------------------------------------------
              SMA-6M * TH3 2C M1 (TAM20/20.Sept.91/PhR)
-----------------------------------------------------------------------------
   NEW FOCAL LENGTH (MM)          =             2520.109406
   VERTEX DISP.(MM)                    DX=  0.000   DY=  0.000   DZ=  0.004
   FOCUS  DISP.(MM)                    DX=  0.000   DY=  0.000   DZ=  0.113
   CENTER OF CURVATURE DISP.(MM)       DX=  0.000   DY=  0.000   DZ=  0.223
   SURFACE ERROR =                       0.984  MICROMETERS R.M.S.
-----------------------------------------------------------------------------
           (dV-dF)/f  Kp(dS-dF)/f   -(Ks/M).dS/f  -(2c/f).Ks.Y/M  TOTAL
(ARC SEC)      0.0        0.0           0.0           0.0           0.0
Rotation about El-axis                                              0.0
M1 mean disp (x,y,z) =      0.000    0.000    -0.009
M2 mean disp (x,y,z) =      0.000    0.000    -0.009
Focus Err=      0.101  Phase Err =     0.016
```

SMA-6M * TH4 2C Y-LIN GRAD (TAM20/20.Sept.91/PhR)

NEW FOCAL LENGTH (MM) =	2519.999992						
VERTEX DISP.(MM)	DX=	0.000	DY=	0.001	DZ=	0.000
FOCUS DISP.(MM)	DX=	0.000	DY=	-0.009	DZ=	0.000
CENTER OF CURVATURE DISP.(MM)	DX=	0.000	DY=	-0.020	DZ=	0.000
SURFACE ERROR =	0.036 MICROMETERS R.M.S.					

	(dV-dF)/f	Kp(dS-dF)/f	-(Ks/M).dS/f	-(2c/f).Ks.Y/M	TOTAL
(ARC SEC)	0.9	-0.2	0.0	-0.1	0.6
Rotation about El-axis					-0.1
M1 mean disp (x,y,z) =	0.000	-0.004	0.000		
M2 mean disp (x,y,z) =	0.000	-0.012	0.000		
Focus Err= 0.000	Phase Err = 0.000				

SMA-6M * TH5 2C Z-LIN GRAD (TAM20/20.Sept.91/PhR)

NEW FOCAL LENGTH (MM) =	2520.053043					
VERTEX DISP.(MM)	DX=	0.000	DY=	0.000	DZ=	0.009
FOCUS DISP.(MM)	DX=	0.000	DY=	-0.001	DZ=	0.062
CENTER OF CURVATURE DISP.(MM)	DX=	0.000	DY=	-0.002	DZ=	0.115
SURFACE ERROR =	0.616 MICROMETERS R.M.S.					

	(dV-dF)/f	Kp(dS-dF)/f	-(Ks/M).dS/f	-(2c/f).Ks.Y/M	TOTAL
(ARC SEC)	0.1	0.0	0.0	0.0	0.1
Rotation about El-axis					0.0
M1 mean disp (x,y,z) =	0.000	0.000	0.005		
M2 mean disp (x,y,z) =	0.000	-0.001	0.001		
Focus Err= 0.054	Phase Err = 0.005				

SMA-6M * TH6 2C M2+QD (TAM20/20.Sept.91/PhR)

NEW FOCAL LENGTH (MM) =	2520.005252					
VERTEX DISP.(MM)	DX=	0.000	DY=	0.000	DZ=	0.000
FOCUS DISP.(MM)	DX=	0.000	DY=	0.000	DZ=	0.005
CENTER OF CURVATURE DISP.(MM)	DX=	0.000	DY=	0.000	DZ=	0.011
SURFACE ERROR =	0.681 MICROMETERS R.M.S.					

	(dV-dF)/f	Kp(dS-dF)/f	-(Ks/M).dS/f	-(2c/f).Ks.Y/M	TOTAL
(ARC SEC)	0.0	0.0	0.0	0.0	0.0
Rotation about El-axis					0.0
M1 mean disp (x,y,z) =	0.000	0.000	0.000		
M2 mean disp (x,y,z) =	0.000	0.000	0.009		
Focus Err= 0.014	Phase Err = 0.020				

SMA-6M * TH7 2C in Ring (TAM20/22.Sept.91/PhR)

NEW FOCAL LENGTH (MM) =	2519.987733					
VERTEX DISP.(MM)	DX=	0.000	DY=	0.006	DZ=	0.014
FOCUS DISP.(MM)	DX=	0.000	DY=	0.019	DZ=	0.002
CENTER OF CURVATURE DISP.(MM)	DX=	0.000	DY=	0.033	DZ=	-0.010
SURFACE ERROR =	0.633 MICROMETERS R.M.S.					

	(dV-dF)/f	Kp(dS-dF)/f	-(Ks/M).dS/f	-(2c/f).Ks.Y/M	TOTAL
(ARC SEC)	-1.1	0.1	-0.1	0.1	-1.1
Rotation about El-axis					-1.1
M1 mean disp (x,y,z) =	0.000	0.008	0.016		
M2 mean disp (x,y,z) =	0.000	0.020	0.017		
Focus Err= 0.004	Phase Err = 0.001				